Sulphur Removal Characteristics from a Commercial NO_X Storage/Reduction Catalyst

by

Darren Scott Kisinger

A thesis
presented to the University of Waterloo
in fulfillment of the
thesis requirement for the degree of
Master of Applied Science
in
Chemical Engineering

Waterloo, Ontario, Canada, 2009

AUTHOR'S DECLARATION

I hereby declare that I am the sole author of this thesis. This is a true copy of the thesis, including any required final revisions, as accepted by my examiners.

I understand that my thesis may be made electronically available to the public.

Darren Kisinger

Abstract

The ability to effectively remove sulphur from sulphur-poisoned NO_X storage/reduction (NSR) catalysts, while minimizing associated fuel penalties and thermal degradation, is important for commercial application of NSR catalysts. As long as sulphur remains in the fuel or lubrication oil formulations, deactivation of NSR catalysts will persist. In an attempt to more fully understand the mechanism of sulphur removal and the associated operating conditions necessary to efficiently decompose sulphates, various gas compositions, temperatures and desulphation methodologies were applied to a commercially supplied catalyst.

Experiments were conducted using a pilot scale plug flow catalytic reactor. FTIR spectroscopy and mass spectrometry were used to measure key sulphur species concentrations. Three groups of experiments were conducted. In the first, the effect of gas composition on the amount of sulphur removed from the catalyst was evaluated. In the latter two, high flow cycling desulphation and low flow cycling desulphation were compared. The most effective desulphation gas composition was achieved through the combination of high concentrations of H_2, CO and C_3H_6 and also the inclusion of CO_2 and H_2O, which released up to 91% of the stored sulphur.

The commercial catalyst tested is designed for a dual-leg process. Dual-leg systems are advantageous over single-leg systems in that engine modifications are unnecessary for catalyst regeneration, thereby minimizing losses in vehicle performance. It was found that under conditions appropriate for that application, catalyst desulphation is dominated by the amount of residual surface oxygen. Through the use of short lean phase cycling, to prevent oxygen saturation, the dual-leg application proved effective for sulphate removal, inducing 69% sulphur release compared to 51% when the surface was saturated with oxygen. Multiple stabilities of sulphur exist on the catalyst, which led to residual catalyst sulphates after many desulphations.

Acknowledgements

I would like to thank Professor William Epling for his professional assistance throughout my graduate research. His knowledge and invaluable insight persistently directed my projects to succeed. It was a privilege to study under his guidance and the opportunity has taught me lasting skills and lessons that I will carry with me throughout my career.

Additionally, I would like to thank NxtGen Emission Controls Inc. for providing the research project. I also would like to acknowledge NSERC for supplying the necessary funding to build the reactor.

Furthermore, I would like to thank Amy for her sincere patience and understanding through all of the late nights and weekends I spent working on this project.

Dedication

I would like to dedicate this work to my parents. This accomplishment would not have been possible without their continued support and encouragement.

Table of Contents

List of Figures

List of Tables

CHAPTER 1: INTRODUCTION

Fossil fuel combustion is the dominant energy production method used around the world. Internal combustion is one such method that has been applied to the industrial, residential and transportation sectors in order to provide energy for processes, home heating and mechanical shaft work. As there is no "clean" combustion process developed for energy production using fossil fuels, there are certain pollutants produced as a result of combustion. According to Environment Canada, the largest emitting pollutant source for nitrogen oxide and nitrogen dioxide (NO_X) in Canada, at approximately 43% of total NO_X released, is from the transportation sector[1]. The production of pollutants such as NO_X, carbon dioxide (CO_2) and sulphur dioxide (SO_2) from combustion processes contributes to the greenhouse effect, the creation of acid rain and to the formation of photochemical smog[2]. Most recently, regulators in the United States have been focusing on reducing the emissions of NO_X, non-methane hydrocarbons (NMHC) and particulate matter (PM) from lean-burn engines (of which the diesel engine is an example) because of increasing global concerns over their environmental impact. Additionally, diesel fuel sulphur content restrictions are currently being employed in the United States to reduce the emissions of SO_X from lean-burn exhaust.

Gasoline powered automobiles have utilized three-way-catalyst (TWC) technology since the mid-1970's in both the United States and Canada. TWC technology has become so advanced that in some metropolitan areas of the United States, the exhaust from a new gasoline powered automobile equipped with super ultra-low emission vehicle (SULEV) technology contains less pollutants than the air injected into the engine[3].

It would seem that since TWC technology has become so advanced, gasoline-powered vehicles would be the obvious choice for transportation use. But in a world of fluctuating, but overall increasing, oil prices the advantage that a diesel vehicle has over a gasoline vehicle is higher fuel efficiency. Since diesel engines have higher fuel efficiency, less CO_2 is released from a diesel vehicle per kilometre travelled compared to that of a gasoline vehicle. The disadvantage with diesel engines is the added challenge of removing PM from the exhaust, whereas gasoline engines do not have this problem. Prior to 2007, US diesel vehicle emission laws were met through either mechanically tuning the engine or by engine modifications. Thus, no wide-spread exhaust after-treatment technology was applied to lean burn engines as of 2007. As legislation to further reduce emissions was proposed in August 2000, engine manufacturers began developing new technologies, including catalyst technologies, to meet the proposed emission targets. Table 1.1 describes emissions regulations set by the United States Environmental Protection Agency for PM, NO_X and NMHC in heavy duty compression ignition vehicles from 1990 to the present[4,5].

Table 1.1 United States Environmental Protection Agency Diesel Emission Standards[4,5]

Year	**$PM_{2.5}$ [g/bhp-hr]**	**NO_X [g/bhp-hr]**	**NMHC [g/bhp-hr]**
Uncontrolled	0.70	--	4.00
1990	0.60	6.0	1.30
1994	0.10	5.0	1.30
1998	0.10	4.0	1.30
Present	0.01	0.20	0.14

The obvious difference between a gasoline and diesel engine is the fuel type used, and therefore their combustion properties are different. This results in the production of different pollutants in the two engine types. Diesel engines run lean, meaning an excess of air is injected into the combustion cylinder with respect to the amount of fuel injected. This type of burn creates an oxygen-rich exhaust stream which contains NMHCs, NO_X and PM. TWCs are designed to operate in environments typical of gasoline exhaust, which is essentially oxygen free due to near stoichiometric combustion; TWCs do not function in an oxidizing, or oxygen-rich, environment. Additionally, TWCs are not capable of removing particulates from diesel exhaust. This lack of functionality in diesel applications has driven significant effort in developing new technologies that work in the oxygen-containing exhaust gas. Fortunately, much of the knowledge gained from the advancement and innovation of TWC technology can still be applied to the emerging lean-burn engine exhaust technologies. New diesel exhaust technologies are currently employed on new production diesel vehicle fleets in both North America and in Europe.

There are several catalytic technologies used for NO_X removal from lean-burn engine exhaust. One is called NO_X storage/reduction (NSR) catalysis, also called a NO_X trap. NO_X traps function by removing NO_X from engine exhaust by collecting and storing NO_X on the catalyst surface. Periodically, when the surface concentration of the catalyst reaches some threshold value, reductant gas is introduced into the exhaust stream via excess fuel injection into the engine and the stored NO_X is released from the catalyst surface and reacts with the reductant to produce nitrogen. Another commercially available technology is selective catalytic reduction (SCR) which uses ammonia, a product of injected urea decomposition, to selectively react with stored exhaust NO_X. A diesel oxidation catalyst (DOC) is set upstream of NSR and SCR catalysts.

DOCs oxidize NO, which is the predominant form of NO_X produced by the engine, into NO_2. NO_2 is preferentially stored on the surface of NSR catalysts, while 1:1 mixtures of NO and NO_2 are preferred for efficient SCR catalyst performance. Particulate filters are used to remove particulates (soot) from engine exhaust.

Many manufacturers are currently using diesel emissions reduction technologies on current auto models. Each company employs a slightly different design that uses one or more of the above emission technologies, each with slight variations such as reductant gas generation methods. These companies include, but are not limited to, Dodge, Mercedes Benz, Volvo, General Motors and BMW. Figure 1.1 shows an exhaust system currently employed on a Mercedes Benz diesel sport utility vehicle (SUV) in the United States. The system on the SUV utilizes all 4 of the diesel exhaust technologies previously described.

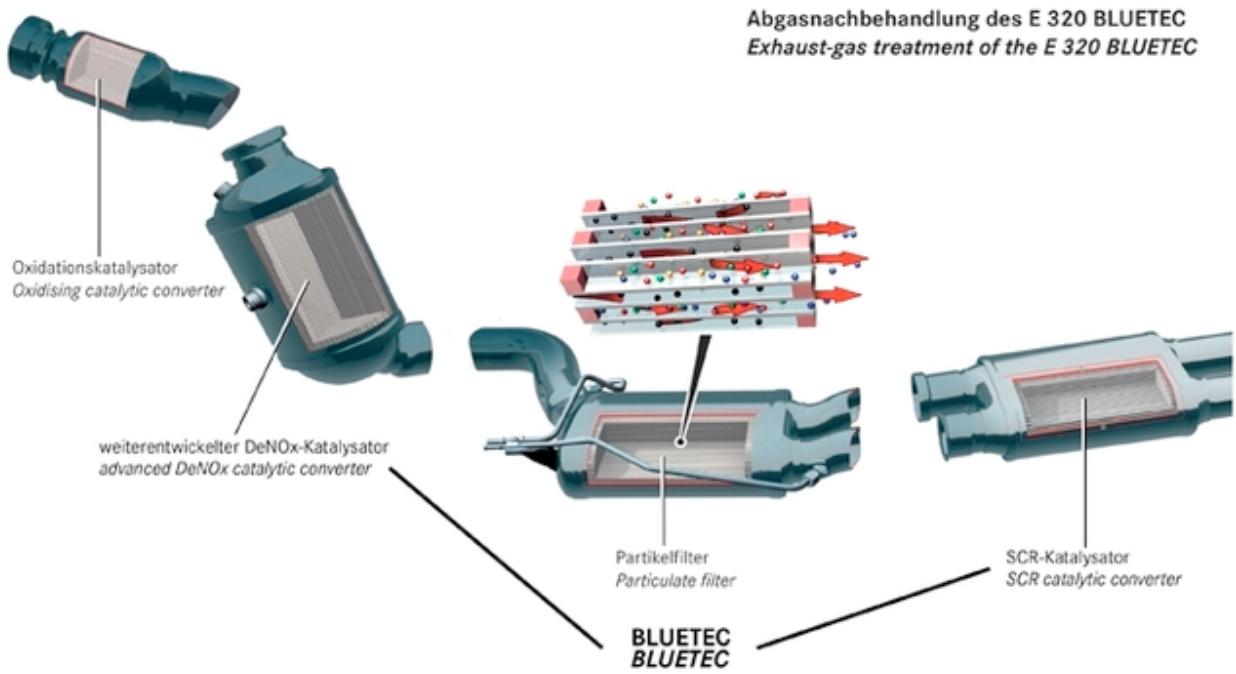

Figure 1.1 Diesel Exhaust System with DOC, NSR, Particulate Filter and SCR[6]

A significant challenge associated with the NSR catalyst technology is the presence of sulphur in the exhaust gas. Sources of sulphur in diesel applications include both diesel fuel and engine lubricating oils. When the sulphur present in the diesel fuel and lubricating oils is combusted in the engine, the main sulphur product is SO_2. The SO_2 poisons trapping sites on the catalysts and over time reduces the catalyst performance to a level that breaches regulatory emission limitations.

Although steps have been taken by the EPA in the United States to reduce the concentration of sulphur in diesel fuel from 500 ppm to 15 ppm[7], the poisoning effect of SO_2 on catalyst systems is still measurable. For example, on a 6 litre NSR catalyst system used on a truck with a 70 litre fuel capacity, a significant increase in NO_X emissions is noticeable after 7 tanks of fuel with 15 ppm sulphur fuel versus 1/5 of a tank of fuel with 500 ppm sulphur fuel. This calculation doesn't take into account the added sulphur from lubricating oils, which have much higher concentrations than the fuel, but lesser amounts are combusted.

As shown by the example, the problem of sulphur poisoning is not eliminated by the reduction of sulphur in diesel fuel, but is only postponed. Poisoned catalytic sites must be regenerated periodically on NO_X traps as long as sulphur exists in the fuel. Removal of the sulphur from a NSR catalyst, called desulphation, requires high temperature with very specific reductant stream gas compositions. One problem with current desulphation techniques is that they require long periods of reductant exposure at high temperatures, which results in large fuel penalties and thermal degradation of the catalyst. In order to maintain diesel vehicle fuel efficiency and the

longevity and activity of NSR catalysts, specific sulphur desorption/reaction temperatures and reductant stream compositions must be understood and applied to existing technology.

NxtGen Emission Controls Inc. is interested in developing technologies to enhance NO_X trap performance for diesel engine applications. They are evaluating an alternate method for catalyst regeneration and desulphation through implementation of their proprietary hydrogen production system.

This thesis presents the analysis of desulphation conditions on the removal of sulphur from a NxtGen-supplied catalyst sample. More specifically, various desulphation temperatures and gas compositions are investigated in order to determine the extent of regained catalytic NO_X performance after each desulphation method. Additionally, the use of a cyclic desulphation technique is compared to that of a constant reductant-rich gas exposure desulphation technique. This is done to evaluate an alternate desulphation method to what is considered the commercial standard.

CHAPTER 2: LITERATURE REVIEW

2.1 NSR Methodology

NSR catalyst systems have proven effective in removing NO_X from lean-burn engine exhaust. The design of the NSR catalyst includes a high surface area washcoat containing a variety of active sites, deposited on a supporting material[8]. The support material is typically a cylindrical honeycomb monolith positioned longitudinally in the tailpipe of a vehicle. Exhaust gases pass through the channels of the monolith and react with the catalyst which is deposited on the channel walls.

The NSR process requires an intermittent switch between two different gas stream compositions. One stream is called the lean phase and is the product of normal lean-burn engine operation. During this phase, NO is oxidized to NO_2, which is stored on the surface of the catalyst in the form of a nitrate. After a period of time, typically the course of several minutes, the surface of the catalyst starts to approach a saturation point in terms of nitrate concentration. An analysis of the outlet gas from the catalyst during the lean phase will show an increasing concentration of NO_X, known as NO_X slip. The second stream, or rich phase, is introduced to the catalyst when some NO_X slip threshold level is reached. The rich phase exhaust gas contains reductants in the form of hydrocarbons, carbon monoxide (CO) and hydrogen (H_2), with little to no oxygen (O_2). The reductants react with the stored nitrates on the catalyst to produce nitrogen, water (H_2O), carbon dioxide (CO_2) and other nitrogen-based compounds. The rich phase is generated by running the lean-burn engine at a sub-stoichiometric ratio for a period of a few seconds. Figure

2.1 shows the NO_X concentration profile downstream of a NSR catalyst through one cycle of operation.

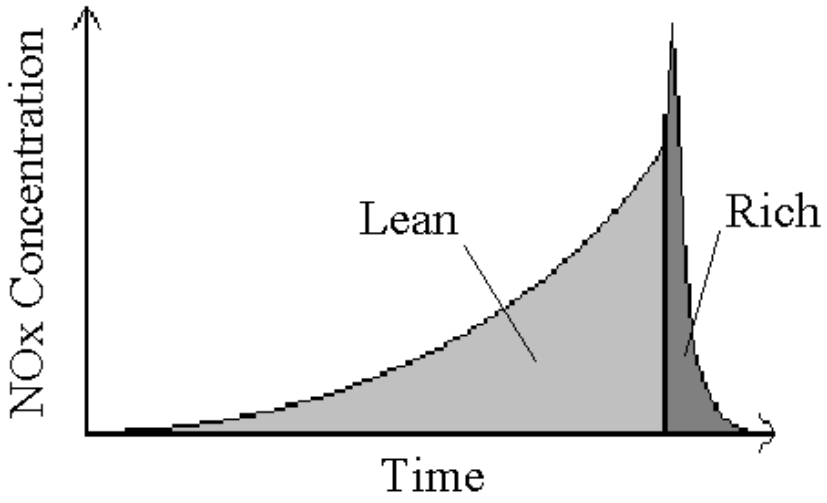

Figure 2.1 Outlet NO_X Concentration Profile During One NSR Cycle

One of the first NSR systems studied is described by Miyoshi et al.[9]. The exhaust stream of a lean-burn gasoline engine was sent through a catalyst composed of platinum, barium and alumina (Pt-Ba-Al_2O_3). During periods of high load conditions, such as acceleration, the vehicle's engine was operated close to stoichiometric. When the vehicle reached cruising speeds, the engine was operated lean. Conditions were alternated between stoichiometric and lean exhaust phases in approximately 2-minute intervals, which the authors suggested would simulate city driving conditions. One of the notable advantages in using this NSR system and mode of operation was that in addition to removing NO_X, engine operation under lean conditions significantly increased fuel efficiency. Soon after this study, other studies found that the lean-to-rich phase timing could be adjusted to increase NO_X removal efficiency. On a prototype

gasoline lean-burn engine, when testing with a 30-second lean and 30-second rich cycle, 94% NO_X removal efficiencies were achieved[10].

The Pt-Ba-Al_2O_3 formulation is common for NSR catalysts[11]. NO_X is composed of acidic NO and NO_2 compounds while the active storage component of such an NSR catalyst is Ba, which is basic. The formation of nitrates on Ba is governed by acid/base chemistry. The actual process by which NO_X reduction occurs over NSR catalysts is very complex and is typically generalized into 5 separate steps which make up the overall reaction mechanism. These 5 steps are NO oxidation, NO_X sorption, reductant delivery and evolution, NO_X release and NO_X reduction[11]. Each step differs in its purpose but all of the steps are important for proper functioning of NSR catalysts.

During the lean phase of lean-burn engine operation, the NO_X in the exhaust gas is mainly in the form of NO, on the order of 90%, with a small amount of NO_2 making up the balance. NSR catalysts trap NO_2 much more readily than NO and so the oxidation of NO to NO_2 is important in the overall NSR reaction mechanism[12]. NO oxidation occurs over the precious metal (Pt) sites on the catalyst via the reaction described in Equation 2.1[12]. The dispersion of the precious metal component has an effect on the extent of NO oxidation. As the precious metal dispersion increases, NO oxidation actually decreases, indicating that this is a structurally sensitive reaction[12]. Temperature of course also affects NO oxidation since it is kinetically limited at lower temperatures, but thermodynamically limited at higher temperatures[13].

$$NO_{(g)} + O\text{-}Pt \rightarrow NO_2\text{-}Pt \qquad (2.1)$$

NO_2 reacts with a Ba complex to form a nitrite/nitrate. As detailed by Hodjati et al.[14] CO_2, H_2O and O_2 exist under actual engine exhaust conditions, and therefore a variety of Ba complexes also exist on the catalyst surface, which include BaO, $Ba(OH)_2$ and $BaCO_3$. Each Ba compound has a different stability, which is a function of temperature. For example, as temperature increases, the stability of $Ba(NO_3)_2$ decreases, such that it decomposes by 480°C[15]. Equations 2.2 to 2.5[11] describe surface reactions between NO_X and the BaO surface complex. It has also been shown that NO_X storage increases with the concentration of O_2[16]. One reason for this is that NO oxidation is promoted with higher O_2 concentration. Additionally, O_2 is required for some of the nitrite and nitrate formation reactions.

$$BaO + 2NO + 0.5O_2 \rightarrow Ba(NO_2)_2 \quad (2.2)$$

$$BaO + 2NO + 1.5O_2 \rightarrow Ba(NO_3)_2 \quad (2.3)$$

$$BaO + 2NO_2 \rightarrow Ba(NO_2)_2 + 0.5O_2 \quad (2.4)$$

$$BaO + 2NO_2 + 0.5O_2 \rightarrow Ba(NO_3)_2 \quad (2.5)$$

Although Ba was used as an example for the storage material of the catalyst, there are other materials used for NSR applications. Alternatives to Ba include alkali earth metals such as K and Na.

Initially, nitrates form on vacant Ba sites at the inlet end of the catalyst. As these sites are saturated, NO_X storage will occur further down the length of the catalyst. After NO_X has accumulated on the catalyst surface and NO_X slip reaches the threshold limit, the NSR system is switched to the reductant-rich phase, which contains reductants such as CO, H_2 (in a 3:1 ratio

with CO[17]) and hydrocarbons but is deficient in O_2. One method to induce the rich phase is to inject extra fuel into the engine and/or decrease the amount of air fed to the combustion cylinder. These adjustments change the A/F ratio in the combustion cylinder so that the combustion reaction is pushed beyond stoichiometric. During the rich phase, the water gas shift (WGS) reaction can also occur over the precious metal sites of the catalyst to produce more H_2 (Equation 2.6)[17,18].

$$CO + H_2O \leftrightarrow CO_2 + H_2 \quad (2.6)$$

The efficient use of reductants for the reduction of nitrates is affected by the oxygen storage capacity (OSC) of the catalyst. In the presence of O_2, reductants will combust over the catalyst. When conditions become rich and no oxygen is present in the exhaust, reductants will still react with stored oxygen on the catalyst. As the OSC of a catalyst increases, the amount of reductant available for NO_X reduction decreases[19]. Consideration of the catalyst OSC is important when determining the length of time to allow for the rich phase in order to ensure enough reductant is delivered for targeted nitrate decomposition and NO_X reduction.

After the evolution and delivery of reductants to the catalyst, stored nitrates on the surface of the catalyst decompose and NO_X is released. This step can be explained by two mechanisms. The first is based on a temperature rise caused by exothermic reductant oxidation of the catalyst OSC. The temperature rise of the catalyst lowers the stability of nitrates on the catalyst and ultimately causes them to decompose[15]. For the second mechanism, at the onset of the rich phase there is a decrease in the amount of NO_X produced from the engine and also a significant drop in the O_2 concentration. The decrease in gas-phase NO_X and O_2 concentrations results in an equilibrium

shift between surface nitrate and bulk gas NO_X and O_2 causing nitrates to decompose [11]. The onset of nitrate decomposition is commonly observable during the rich phase by a NO_X concentration spike from the outlet of the catalyst, as shown in Figure 2.1. The spike occurs as a result of inadequate reductant delivery to fully reduce the large amounts of NO_X initially released.

The final step of the NSR mechanism is the reduction of NO_X, formed by nitrate decomposition, to nitrogen (N_2). Two mechanisms have been proposed for this reaction step. The first proposes that NO_X decomposes on precious metal sites of the catalyst to Pt-N and Pt-O and then Pt-N sites combine together with each other to form N_2[20]. The Pt-O sites react with reductants to form H_2O and CO_2. Undesired products can be generated as well, including N_2O from the reaction of NO with Pt-N, and NH_3 from the reaction of Pt-N with H_2[20]. The second proposed mechanism suggests that the reductant is activated on Pt sites, so that it reacts directly with nitrates to produce N_2[21]. Since neither reaction mechanism has been confidently proved or disproved, both mechanisms continue to be considered.

In summary, operation of a NSR catalyst involves 5 reaction steps; NO oxidation, NO_X sorption, reductant delivery and evolution, NO_X release and NO_X reduction. As will be discussed, the key reaction affected by sulphur poisoning is NO_X sorption, due to similarities between the SO_2 and NO_2 reactions on catalyst storage sites.

2.2 NSR Design

The supporting honeycomb monolith is designed to handle the mechanical stresses due to driving, provide the maximum geometric surface area and promote the heat transfer necessary to sustain high temperature reactions[3]. In many vehicles, the supporting material is ceramic, typically cordierite, which provides desirable thermal properties. Supports are also designed to minimize the pressure drop across the catalyst, since any back pressure on the engine can reduce the power of the vehicle[3]. There are many other design properties associated with supporting materials, but they are not fundamental to the performance of NSR systems.

The honeycomb monolith support is covered by a washcoat phase which provides a high surface area over which the active sites are dispersed, thereby increasing their exposure to reactant gases. The washcoat typically consists of a matrix of macro-, meso- and micro-pores providing the high surface area. The most common washcoat material used for NSR catalysts is γ-alumina (γ-Al_2O_3). γ-Al_2O_3 has a surface area typically between 150 – 300 m^2/g and has strong resistance to thermal aging. A study by Shimizu et al.[22] on the NSR compared the use of MgO, ZrO_2 and SiO_2 washcoats to that of Al_2O_3. The order of NO_X saturation from highest to lowest was found to be MgO, Al_2O_3, ZrO_2 and SiO_2. Decreasing NO_X storage order was associated with increasing washcoat acidity. Although the MgO washcoat catalyst proved to have the highest NO_X storage capacity, the used of the Al_2O_3 washcoated catalyst resulted in far greater NO_X reduction likely due to better dispersion of the active metal sites, as will be described below. Casapu et al.[23] demonstrated an Al_2O_3-washcoated catalyst stored and reduced NO_X better compared to a CeO_2-washcoated catalyst. Although γ-Al_2O_3 washcoats are still the most

commonly used in NSR catalysts, research continues at finding a material more suited for NSR catalyst applications. One such washcoat recently described is a nanocomposite of Al_2O_3 doped with ZrO_2-TiO_2, designed to better withstand the poisoning effects of sulphur[24].

NSR catalysts must oxidize NO, store NO_X and also release and reduce the stored NO_X to N_2. This complex series of functions tends to limit the choice of catalyst metals for NSR applications. For the oxidation of NO, precious metal catalysts such as Pt and Pd are typically used[25]. The cost of the precious metal component has a large impact on the catalyst manufacturer design, since it typically accounts for the largest portion of catalyst cost. For NSR applications, too much precious metal on the catalyst can actually have adverse effects on catalyst performance. For example, at lower loadings, as the amount of Pt increases, so does the rate of NO oxidation. However, if the Pt loading is increased too much, Pt-catalyzed nitrate decomposition will begin during the lean phase, which will reduce nitrate storage capacity[26]. The optimum precious metal loading must be pre-determined experimentally in order to maximize NO oxidation and eliminate nitrate decomposition during the lean phase.

Alkali and alkaline earth metals are typically used as the catalyst trapping component since they are basic in nature and will react with acidic NO_X to form nitrite and nitrate species. There are many choices for alkaline earth storage materials, including Ca, K, Na, Ce, Ba and Mg[27]. Ba is commonly used in NSR catalysts due to its ability to store NO_X between 250^{o}C and 450^{o}C. K has more potential for higher temperature NSR systems since it can store NO_X up to 550^{o}C. Unfortunately, K is very reactive with Pt and can inhibit NO oxidation[26]. This downside has limited its use in NSR systems. Another characteristic that is essential when choosing the

catalyst storage metal, other than the ability to trap NO_X, is also the ability to release nitrates during the regeneration period. Previous work has shown that this is related to nitrate stability which decreases in the order K > Ba > Na > Ca > Li, for these components[28].

The choice of NSR catalyst oxidation and trapping components, washcoat and supporting material are not the only aspects of NSR design that are frequently considered and researched. Methods for the generation of reductant have also been studied. As previously mentioned, the generation of reductant for the rich phase can be accomplished by running the engine rich where the A/F ratio (lambda) is changed to achieve stoichiometric combustion and generate reductants. Minimizing changes to lambda is desirable for some applications. For example, in retro-fit applications, engine modifications would be too expensive, and therefore reductant generation is accomplished through the use of secondary fuel injectors downstream of the engine[29]. This directly injected fuel is partially oxidized over the catalyst to produce reductant gases which then react with stored nitrates on the catalyst. The problem with injecting fuel directly into the lean-burn exhaust stream is that a large portion of the fuel will be combusted with the oxygen. This reduces the use efficiency of the fuel to reduce nitrates[30] and creates large exotherms on the catalyst which can lead to thermal degradation. An alternate method to generate reductants includes using an upstream fuel reformer to convert fuel to H_2[31] implemented in a 2-leg system. A 2-leg, or dual leg, design is shown in Figure 2.2 and further discussed below.

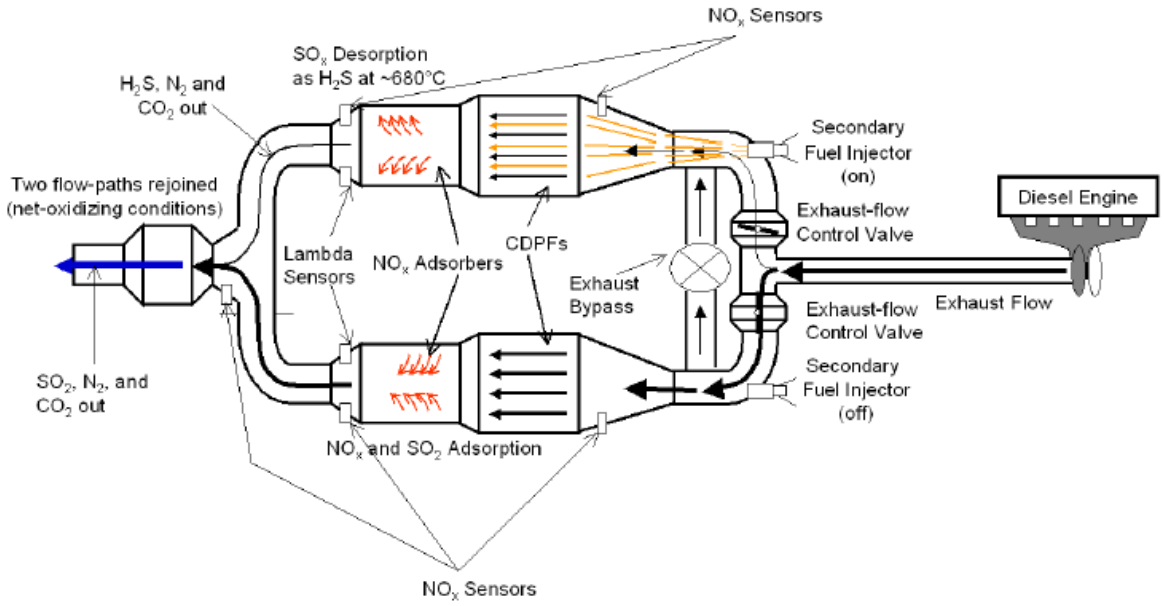

Figure 2.2 Diagram of a Dual Leg NSR Catalyst System[29].

Dual leg systems use two catalysts arranged in parallel such that one is exposed to the bulk of the engine exhaust, matching the lean, or trapping, phase described above. A small portion of the exhaust, as well as reformed fuel, is directed to the catalyst being regenerated. The inclusion of a small portion of hot engine exhaust to the regenerating catalyst serves to maintain the temperature of the catalyst during reduction and carry the injected reductant through the catalyst. The advantage to a dual leg system is that the engine does not have to switch between lean and rich phase operation. This maintains high engine efficiency and also minimizes the combustion of injected fuel with exhaust O_2 since only a small portion of exhaust is directed through the regeneration side. This results in better fuel efficiency compared to direct reductant injection in a single-leg system.

2.3 NSR Deactivation Mechanisms

NO_X conversion will decrease over time through a variety of degradation modes. There are two specific deactivation mechanisms that contribute to the performance loss: thermal degradation and poisoning, although the effects of masking and attrition will also be discussed for completeness.

Attrition is the erosion of catalyst materials due to friction. For NSR monoliths, attrition is minimized due to the fact that the only mechanical friction occurs between the gas and the catalyst. These gas-solid friction forces are not great enough to remove catalyst particles at any measurable rate. Attrition of NSR catalysts can also occur as a result of solid-solid interactions. Solid-solid attrition typically results from the thermal expansion and contraction of the support and washcoat material to different extents as the catalyst is heated and cooled, possibly resulting in detachment of the washcoat from the ceramic support[3]. Presently, NSR catalysts are designed so attrition degradation is negligible with respect to other deactivation mechanisms.

Masking is also not considered problematic in NSR catalysts. Masking occurs when particles build-up on or clog pores on the surface of the catalyst, thereby covering or blocking access to active catalyst sites and reducing the reactivity of the catalyst. Particulate matter produced by lean-burn engines does not have a tendency to "stick" to the catalyst surface and so it does not pose a significant problem[3].

Thermal degradation of NSR catalysts is a problem as high temperature exposures are necessary under certain conditions. The exposure to high temperatures affects the support, the washcoat and catalyst metals in different ways. A decrease in NSR performance is a direct result of thermal degradation[32].

Large temperature swings can cause cracking of the ceramic support, which can block monolith channels. Extensive testing must be carried out on monoliths for vehicle applications to determine the resistance to thermal shock and cracking. Although uncommon in modern catalysts, support failure can be an issue if inadequate thermal testing is conducted on new monoliths[33].

With exposure to high enough temperatures, the catalyst washcoat surface area will decrease irreversibly. In the case of Al_2O_3, thermal degradation results in solid-phase transitions which yield a lower surface area. The γ-Al_2O_3 phase has the highest surface area, between 150 - 300 m^2/g[34], while Θ-Al_2O_3 has a lower surface area and α-Al_2O_3 has the lowest surface area of about 5 m^2/g. As demonstrated by Loong et al[35], the intermediate Θ-alumina phase began to form at temperatures as low as 600^oC. A 90% phase transition to α-alumina occurred at 1175^oC. The addition of rare-earth compounds to Al_2O_3 can inhibit thermal degradation. The same researchers showed that the addition of La to the Al_2O_3 washcoat shifted the 90% phase transition of γ-Al_2O_3 to α-Al_2O_3 from 1175^oC to 1300^oC. Although this shift was observed far above the temperatures encountered in lean-burn engine exhaust, the results show the potential to increase the thermal stability of Al_2O_3 through the addition of a rare-earth compound or other additives.

Thermal degradation also causes sintering, or clumping, of the catalyst precious metal components. Pt sintering occurs under both oxidizing and reducing conditions, although is typically faster under oxidizing conditions[36]. The increased sintering severity under oxidizing conditions is due to the formation of Pt-O which is more mobile and therefore clumps together faster[37]. Lee and Kung[38] have shown that as sintering increases and clumping/particle size increases, NO oxidation over NSR catalysts increases, suggesting that NO oxidation is a structure-sensitive reaction. Further analysis of the structural sensitivity of NO oxidation by Olsson and Fridell[37] suggested that large Pt particles are more difficult to oxidize than smaller particles since the metal catalyzes the reaction, this leads to higher rates of NO oxidation. However, if the catalyst is exposed to a high enough temperature, severe sintering will occur and NO oxidation will ultimately decrease. To slow the rate of precious metal sintering, Ce is often added to such catalysts. Oxides of metals such as Ce decrease the ability of other metals to migrate over the catalyst surface[39].

Thermal aging also has an effect on the Ba storage sites. According to Kim et al.[40], thermal aging of a BaO/Al_2O_3 sample at 1000°C resulted in the formation of $BaAl_2O_4$. $BaAl_2O_4$ does not have the ability to form nitrate salts and therefore results in a NO_X storage loss. The addition of water to the exhaust gas mixture during thermal aging resulted in the formation of large $BaCO_3$ crystallite structures on both BaO and $BaAl_2O_4$ surfaces. As with $BaAl_2O_4$, large $BaCO_3$ crystals do not possess the ability to form nitrates. When these form, the NO_X storage capacity of the catalyst is therefore further reduced. In another study by Kim et al.[41], some of the storage activity of the catalyst was regenerated through the adsorption of NO_2 and subsequent room temperature water exposure. During room temperature water exposure, $BaAl_2O_4$ species

underwent a phase change to $Ba(NO_3)_2$ crystals. After heating to 750°C in inert conditions, $Ba(NO_3)_2$ crystallites decomposed, restoring the active Ba site. This regeneration technique is however rather difficult to apply to mobile automotive technologies and is more suitable for stationary applications. Another effect of thermal aging is Ba sintering. Above 600°C, clumping of Ba particles can occur as a result of increased Ba surface mobility[42]. This Ba agglomeration decreases the number of available nitrite/nitrate storage sites on the catalyst by decreasing the surface area of Ba particles exposed to the gas. The severity of Ba clumping increases with increasing temperature and can be reduced through the addition of metals which decrease surface migration, such as Ce[39].

The last deactivation mechanism to be discussed is sulphur poisoning, which along with its effects on NSR catalyst activity, is the focus of this thesis. As previously mentioned, sulphur is present in diesel fuel and lubricating oils. With new EPA regulations, the concentration of fuel sulphur in the U.S. is 15 ppm[7]. In comparison, the lubricating oils of the engine contain between 2500 ppm to 8000 ppm depending on the oil quality. The lubricating oil sulphur concentration corresponds to an approximate maximum equivalent fuel concentration of 7 ppm of SO_2 in the exhaust[43]. Figure 2.3 presents the severity that sulphur deposition on the catalyst has on the ability of NSR catalysts to convert NO_X.

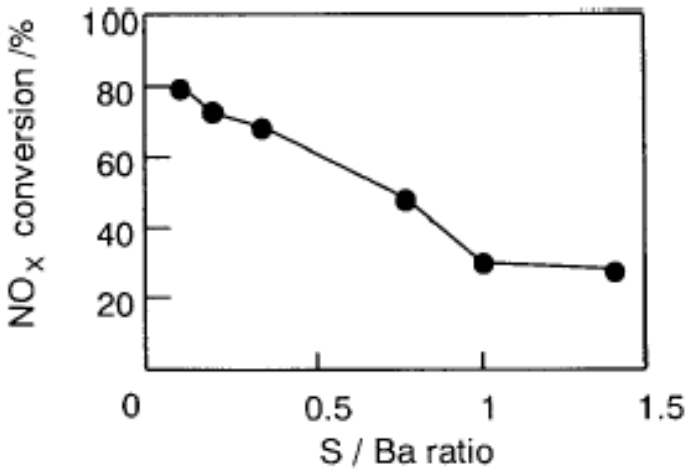

Figure 2.3 Effect of Sulphur Deposition on NO_X Conversion[44]

Sulphur poisoning occurs through the oxidation of SO_2 and subsequent sulphate formation on Ba or other NO_X trapping sites. Sulphate formation blocks sites that would otherwise form nitrates. Since sulphates are much more stable than nitrates, they are more difficult to remove from the catalyst. $BaSO_4$ does not decompose within the normal temperature range of lean-burn engine exhaust. Even at high temperature, the exhaust gases must be rich in reductant to remove $BaSO_4$. Such conditions result in high fuel consumption. Additionally, high temperatures result in the thermal degradation of the catalyst.

One method to avoid this type of catalyst poisoning is the use of upstream sulphur traps, which remove sulphur from the exhaust stream prior to reaching the NSR system. In one study, when exposed to a large sulphur load over a prolonged period of time, the performance of a NSR system equipped with a sulphur trap retained approximately 80% of its original NO_X conversion compared to 20% retention in its absence[45]. There is however complications associated with using sulphur traps. A sulphur trap cannot function indefinitely without having to be

regenerated. Upon periodic regeneration, unless exhaust gas is directed elsewhere, the outlet from the sulphur trap can severely poison the NSR catalyst downstream. Additionally, sulphur traps can act as heat sinks, thereby delaying NSR catalyst warm-up or lowering the overall NSR catalyst operating temperature. A final downside to sulphur traps is that they add additional costs and space requirements to the NSR system. Until sulphur is completely eliminated from fuel and lubricating oils in diesel vehicles, it will pose a persistent and recurring problem for NSR catalysts.

2.4 Sulphur Deactivation Chemistry

It is important to know and understand under what conditions sulphur poisoning occurs and when or how frequently it is necessary to perform a procedure to remove the sulphur. Sulphur poisoning affects the catalyst in both lean and rich conditions, although with more severity during rich[46]. Sulphur poisoning affects all NSR catalyst components[46], but Ba is most affected. The poisoning effect on Ba causes higher levels of NO_X slip earlier in the lean cycle of operation. Therefore in order to maintain some level of NO_X conversion, regeneration must occur more frequently leading to higher fuel penalties. Engstrom et al.[47] demonstrated that the loss of NO_X conversion increases in an approximately linear relation with total sulphur dose. This is expected as sulphur occupies active catalyst trapping sites in a 1:1 ratio with Ba. Because of this linear decrease in performance, NSR systems are designed to operate until the catalyst is exposed to a threshold amount of sulphur, at which time a sulphur removal procedure, known as a desulphation, is triggered.

The main form of sulphur that exits the engine is SO_2, but hydrogen sulphide (H_2S) and carbonyl sulphide (COS) are also present in smaller quantities during the lean phase and higher concentrations during rich conditions. Poisoning by H_2S, COS or SO_2 leads to slightly different extents of deactivation, with SO_2 having the more significant effect[46]. Since there is only a small difference in the extent of poisoning between sulphur compounds, and because SO_2 is the main sulphur product from the engine, SO_2 is typically used in laboratory experiments to investigate NSR poisoning effects.

A great deal of research has been directed at understanding the poisoning mechanism of Ba sites. Sulphur poisoning on Ba occurs similarly to NO_X storage and nitrate formation during lean conditions, only that SO_2 stores preferentially and sulphates are more stable than nitrates. SO_2 is oxidized on the Pt sites with O_2 forming SO_3. Depending on the pre-existing surface Ba complex, the SO_3 complex further reacts to produce H_2O or CO_2 and $BaSO_4$[48]. The evolution of H_2O, as observed by De Wilde and Marin[48], when SO_2 was exposed to a NSR catalyst demonstrates the replacement of the hydroxide from $Ba(OH)_2$ with SO_3 to form $BaSO_4$. Additionally, the evolution of NO_X from catalysts during lean conditions has been observed during exposure to SO_2[47]. These observations imply that SO_2 is preferentially trapped relative to NO_X. Again, once sulphates are formed, these sites can no longer participate in NO_X trapping until the sulphates are removed.

Ba sites are not the only sites on the catalyst that are deactivated by sulphur. Fridell et al.[49] reported that sulphur poisons Pt sites during the rich phase through formation of Pt-S. During lean conditions, sulphur that adsorbs on Pt is oxidized due to the high availability of O_2. Pt-S

formation during the rich phase can affect the NO oxidation ability of Pt at the beginning of a subsequent lean phase since it will not occur on the Pt-S complex until the sulphur atom is oxidized off. During this time, the NO oxidation ability of the catalyst is reduced and a reduction in NO_X storage may result. An additional consequence of Pt poisoning is that sulphur can cause increased mobility of Pt on the catalyst surface[49]. This phenomenon can promote Pt sintering at high temperatures and is a considerable problem during desulphation as it enhances thermal degradation.

Sulphur poisoning of the alumina washcoat follows a similar mechanism as that of Ba. SO_2 is oxidized over Pt and is stored on Al_2O_3 in the form of an alumina sulphate ($Al_2(SO_4)_3$)[50]. Sulphur poisoning of alumina does not directly affect the ability of the NSR catalyst to convert NO_X to N_2, but when a desulphation procedure is conducted the sulphur that is removed from the Al_2O_3 may re-adsorb onto an adjacent un-poisoned Ba site or one downstream[32]. Sulphur re-adsorption will increase the necessary time for desulphation, which increases fuel penalties and the extent of thermal degradation.

Typically the highest concentration of sulphates is found just after the inlet to the catalyst[51] where SO_2 is first oxidized and subsequently stored. The same principle holds for NO_X and stored nitrates. As sulphates form in the place of nitrates, a reduction in NO_X performance is observed relatively quickly. The discharge end of the catalyst, which is typically poisoned last, can continue to perform when the front end is poisoned. However, since the discharge end of the catalyst does not receive as much heat as the front end[33], this contributes to NO_X performance reduction when trapping and reduction activity is restricted to the rear of the catalyst. There is of

course also an effect on reaction residence time. With more NO_X trapped downstream, the released NO_X has less catalyst downstream for the reduction reaction during the rich phase. This typically results in more release during the rich phase and higher amounts of N_2O by-product[52].

2.5 Sulphate Decomposition

As a result of sulphur poisoning, catalysts must be periodically regenerated by removing the sulphur, to restore NO_X conversion performance. In order to develop an effective desulphation strategy, it is important to understand what temperatures and gas compositions induce sulphate decomposition and sulphur release. To determine these reaction conditions, a technique known as temperature programmed reaction (TPR) is often employed. To perform a TPR experiment, a specific quantity of sulphur is first deposited on the catalyst at low temperature. The temperature is then increased at a specified ramp rate in the gas mixture to be evaluated. The concentrations of species that are released during the heat ramp are constantly recorded. This will identify the reaction temperatures where deposited sulphates decompose. Gas stream concentrations and compositions can be varied among multiple TPRs in order to determine which gas stream causes sulphate decomposition at the lowest temperature.

One such TPR experiment was performed by Ura et al.[53]. After a fixed quantity of sulphur was deposited on the catalyst, the sample was exposed to a rich gas mixture containing a 3:1 ratio of CO to H_2, along with CO_2 and H_2O. SO_2, H_2S and COS were released from the catalyst under these conditions. The release of SO_2 from the catalyst was observed between 400^oC and 540^oC, while the release of H_2S and COS occurred at higher temperatures up to 800^oC. This large

temperature range indicated varying levels of sulphate stability. These different stabilities correspond to different sulphate complexes and/or to the formation of sulphates on different catalyst components. $BaSO_4$ is the typical sulphate that is formed on Ba sites. Another sulphur complex that can be formed on Ba under appropriate conditions is BaS. BaS is the most stable form of sulphur stored on the NSR catalyst. The sulphide complex has been shown to remain to temperatures above 800°C[54,55]. Since such a wide range of sulphur complexes and stabilities can form on the catalyst, each with its own decomposition temperature, understanding which desulphation gas compositions lower reaction temperatures is essential to minimizing thermal degradation and the fuel penalty associated with desulphation.

In contrast to exposure to constant reducing conditions, many desulphation procedures include frequent cycling between lean and rich phases. This maintains catalyst desulphation temperature through the exothermic combustion of reductant with catalyst OSC and lean/rich interface O_2, and permits the re-oxidation of Pt-S sites which may accumulate when conditions are continually rich. Molinier[56] however demonstrated that a constantly reducing desulphation environment is more effective in removing sulphates from the catalyst than lean/rich cycling. However, the application of a prolonged rich phase in diesel vehicles is not desirable because of the associated high fuel penalty and inability of the diesel engine to burn rich for such a long time, as well as the mentioned need to increase the catalyst temperature.

A standard desulphation gas composition described by Ura et al.[53] is the combination of CO, H_2, CO_2 and H_2O. H_2 is more effective than CO for reducing sulphates on the catalyst surface[32,55]. However, reductants are not effective without Pt[57]. This suggests that Pt

participates in sulphate reduction reactions through the activation of either the reductant or the sulphate species. The effect of H_2O addition on the desulphation gas mixture is also beneficial. BaS forms from the reaction of $BaSO_4$ with H_2 at temperatures as low as 550°C[27,54,55]. Since BaS is the most stable form of sulphur on the catalyst, the production of BaS is an extremely undesired reaction. The presence of H_2O in the reducing stream hydrolyzes BaS to BaO (Equation 2.7[54]), thus preventing the accumulation of BaS on the catalyst. Additionally, Chang[58] showed that the presence of water reduces the degree of washcoat sulphur poisoning.

$$BaS + H_2O \rightarrow BaO + H_2S \qquad (2.7)$$

When CO is used as a reducing agent in the presence of water, excluding CO_2 and H_2, small amounts of COS are produced from the catalyst surface at high temperatures (1000°C)[19,59]. The addition of CO to a desulphation gas mixture containing H_2, H_2O and CO_2 reduces desulphation reaction temperatures further. This is believed to be due to increased H_2 produced via the WGS reaction[19]. The addition of CO_2 to the desulphation gas stream in the presence of H_2 and H_2O reduces the necessary desulphation temperature[55]. In summary, literature evidence shows it is most effective to use a combination of CO_2, H_2O, H_2 and CO to reduce sulphates from Ba sites. Also, the inclusion of H_2O in the desulphation gas stream is essential to prevent the retention of BaS on the catalyst.

Another technique used to minimize the formation of sulphates on the catalyst and reduce the temperature of sulphate decomposition involves the addition of promoters such as Rh[50]. Rh-ZrO_2 deposited on the NSR catalyst promotes the generation of H_2 through the steam reforming

reaction[17,44]. Alternatively, Ce addition to NSR catalysts reduces the degree of poisoning on Ba sites since sulphates can form on Ce sites instead of Ba sites[50].

Many different alkali and alkali-earth metals have been investigated for NO_X storage in place of Ba. Some of these storage metals release sulphur at lower temperatures[27,32]. The problem with alternative storage materials is that both nitrate and sulphate reactions are similar and are governed by acid/base chemistry. As the ability to store SO_2 decreases, so does the ability to trap NO_X. For example, Li has the ability to store nitrites/nitrates/sulphates at lower temperatures than Ba[27,32]. As a result, sulphate decomposition on Li occurs at lower temperature, potentially increasing the amount of recoverable activity of the catalyst after low-temperature desulphation procedures. Unfortunately, decomposition of nitrites/nitrates on Li also occurs at lower temperatures, reducing the storage ability of the catalyst at higher temperatures. The opposite is true for materials that are more basic than Ba. For example, Monroe and Li[60] demonstrated the difficulty in removing sulphur from a K-based catalyst. Since K nitrate is more stable than Ba nitrate, this effect leads to increased sulphate stability. Kim et al.[61] investigated the effect of Ba loading on the ease of sulphur reduction and showed that higher sulphur removal rates occurred with lower Ba loadings. This was attributed to the fact that lower Ba loadings resulted in the formation of a structural monolayer of sulphates, which were easily accessible for reduction in comparison to multilayer sulphate formation at higher Ba loadings.

Although extensive research is being conducted on desulphation procedures, the problem of sulphur poisoning has yet to be resolved. One of the largest difficulties associated with sulphur is that once a NSR catalyst has been poisoned, it is difficult to fully regenerate the catalyst due to

the formation of very stable sulphates[55,61]. Procedures that attempt to achieve full removal of sulphur from the catalyst result in severe thermal degradation. There is simply no published desulphation strategy that fully regenerates NSR catalysts without resulting in significant degradation or a large fuel penalty.

CHAPTER 3: EXPERIMENTAL DESIGN

3.1 Catalyst Characterization

The catalyst sample tested was supplied by NxtGen Emissions Controls Inc. The catalyst was 7.5 inches in diameter and 5 inches in length. The measured monolith cell/channel density was approximately 300 cells per square inch. Samples were cored from the catalyst block for testing. Each tested catalyst sample was identical in dimension and cell/channel count. Cored catalyst specimens were 0.77 inches in diameter and 3 inches in length. The cell count of each specimen was 138 cells. The dimensions of the catalyst samples were calculated prior to coring in order to achieve a 55 000 hr^{-1} space velocity for high flow experiments, to be described below. This corresponded to a 20.84 L/min flow rate. The mass of the cored and dimensioned samples was approximately 17.1 grams per sample. Details of the catalyst washcoat and metal composition were not disclosed by NxtGen Emission Controls Inc. and are therefore not discussed.

3.2 Experimental Apparatus

A pilot scale plug flow reactor (PFR) was used to test the NxtGen catalyst. Exhaust gases were fed to the reactor using mass flow controllers (MFCs). Reactor outlet gas analysis was conducted using a MKS 2030 Fourier Transform Infrared (FTIR) multi-gas analyzer and a Hiden Analytical Mass Spectrometer. The PFR is limited to operating temperatures between 25^{o}C to 950^{o}C and a 0.515 L/min lower flow rate. A detailed process and instrumentation diagram (P&ID) for the PFR can be found in Appendix A, Figure A.1.

The gases used were supplied by compressed gas cylinders purchased from PraxAir Inc. The gases were nitrogen (N_2), helium (He), oxygen (O_2), carbon dioxide (CO_2), hydrogen (H_2), propylene (C_3H_6), carbon monoxide (CO), nitric oxide (NO) and sulphur dioxide (SO_2). Gases were supplied to MFCs at 45 psi (310.26 kPa). The outlet pressure from each MFC was atmospheric. Two mixing manifolds were used; manifold 1 was used for the lean gas mixture, while manifold 2 was used for the rich gas mixture. MFCs supplied N_2, O_2, NO and SO_2 to manifold 1. N_2, C_3H_6, H_2 and CO were supplied to manifold 2. Downstream of the mixing manifolds was a 4-way actuated switching valve. The actuation of the switching valve was powered with compressed N_2 at 75 psi (517.1 kPa). The switching valve was used to alternate between gases from manifold 1 and manifold 2 to the reactor. The stream not fed to the reactor was simply vented to the lab exhaust. CO_2, H_2O and He were introduced downstream of the 4-way switching valve.

A gas pre-heating system consisting of a line heater and insulation tape wrapped around a tubing coil, located downstream of the switching valve and CO_2/He injection point, was used to heat the gas to approximately 150^{o}C. The water vapour injection point was located at the outlet of the pre-heated gas coil. Water was injected, along with a N_2 gas carrier stream, through a Bronkhorst evaporator system. Downstream of this junction, the gases passed through an oxygen sensor and then on to the quartz tube reactor. The exhaust gas mixture temperature was maintained between 140^{o}C and 150^{o}C up to the quartz tube reactor inlet using line heaters and insulation in order to prevent water condensation in the tubing.

The inlet of the quartz reactor tube, 1" inner diameter, was filled with smaller quartz tubes. These smaller tubes added a high surface area for conductive heat transfer from the furnace to the gas stream. The catalyst was located downstream of these tubes. Vermiculite insulation was wrapped around the catalyst to prevent gas bypass around the catalyst sample. The quartz reactor tube was placed in a Lindbergh programmable tube furnace.

After exiting the reactor, the exhaust gases passed through another oxygen sensor and were directed to the FTIR gas analyzer and mass spectrometer, which measured the outlet gas compositions. Temperatures were measured at various sampling points in accordance with the pre-referenced P&ID, using K-type thermocouples.

All tubing, fittings and valves other than the reactor tube itself were made from stainless steel. All heated sections of the reactor were insulated with insulation tape.

3.3 Experimental Procedure

Three specific categories of desulphation experiments were conducted. In the first set of experiments, the sample was exposed to SO_2 at 300^{o}C, heated to 600°C in an inert phase and then continuously exposed to a rich phase. This was done several times with different gas-phase compositions to determine the effect of the desulphation gas composition on the extent of sulphur removal. In the second set, cycling desulphation experiments were run after sulphur exposure at 300°C, with both lean and rich phases, at a flow rate of 20.84 L/min and at four different temperatures (500, 550, 600 and 650°C). A similar set of cycling desulphation

experiments was conducted but at a lower flow rate of 0.515 L/min at the same temperatures for comparison. This lower flow rate simulates those used in a 2-leg system during desulphation.

The main purpose of the experiments was to determine the optimal operating conditions for sulphur removal from the NxtGen catalyst in a dual-leg NSR design and compare the results to conditions that are similar to a single-leg commercial NSR design. The high flow cycling tests represent current commercial NSR desulphation methodology whereas low flow cycling desulphation simulates that of a 2-leg system. Each category of desulphation experiments, as well as specific details of the desulphation experiments, is described in detail in the sections to follow. A complete list of experiments conducted can be found in Table 3.1 below.

Table 3.1 Complete List of Desulphation Experiments

Flow Rate [L/min]	**Method**	**Cycles [#]**	**Temperature [^{o}C]**	**Experiment Description**
20.84	Cycling	29	500	Table 3.5 Lean/Rich = 5/20 Seconds
20.84	Cycling	29	550	Table 3.5 Lean/Rich = 5/20 Seconds
20.84	Cycling	29	600	Table 3.5 Lean/Rich = 5/20 Seconds
20.84	Cycling	29	650	Table 3.5 Lean/Rich = 5/20 Seconds
20.84	Continuous	0	600	Table 3.4 High 1 for 12 Minutes
0.515	Cycling	29	500	Table 3.6 Lean/Rich = 90/20 Seconds
0.515	Cycling	29	550	Table 3.6 Lean/Rich = 90/20 Seconds
0.515	Cycling	29	600	Table 3.6 Lean/Rich = 90/20 Seconds
0.515	Cycling	29	650	Table 3.6 Lean/Rich = 90/20 Seconds
1.029	Cycling	29	600	Table 3.6 Lean/Rich = 90/20 Seconds
0.515	Cycling	29	600	Table 3.6 Lean/Rich = 90/20 Seconds
0.515	Continuous	0	600	Table 3.4 Low 1 for 12 Minutes
0.515	Continuous	0	600	Table 3.4 Low 2 for 12 Minutes
0.515	Continuous	0	600	Table 3.4 Low 3 for 12 Minutes
0.515	Continuous	0	600	Table 3.4 Low 4 for 12 Minutes

Prior to actual catalyst testing, the sample was degraded at 700°C in a flowing stream of 10% H_2O, 21% O_2 and 69% N_2 for 10 hours. This prevented changes in the degree of thermal degradation between desulphation experiments. To begin each individual experiment, the sample was conditioned at 500°C, in a gas stream at 20.84 L/min containing 1% H_2, 6% CO_2, 7% H_2O and 86% N_2 for 15 minutes. After conditioning, the gas stream was changed to the composition shown in Table 3.2, but excluding SO_2, and cooled to 350°C. Note that the N_2 balance makes up for the missing SO_2 flow in the gas stream to preserve the desired compositions. At 350°C, NO_X cycling tests were performed using the gas compositions described in Table 3.3. Lean cycle phase times were 30 seconds and rich phase times were 5 seconds. All NO_X cycling experiments were conducted at 350°C with a flow rate of 20.84 L/min and the gas compositions described in Table 3.3.

Table 3.2 Sulphur Exposure Experimental Flow Composition

Gas Stream	SO_2 [ppm]	H_2 [%]	CO [%]	C_3H_6 [%]	CO_2 [%]	H_2O [%]	O_2 [%]	He [%]	N_2
Sulphur	95	0	0	0	6	7	10	1	Balance

Table 3.3 NO_X Cycling Experimental Flow Compositions

Gas Stream	NO [ppm]	H_2 [%]	CO [%]	C_3H_6 [%]	CO_2 [%]	H_2O [%]	O_2 [%]	He [%]	N_2
Lean	250	0	0	0	6	7	10	1	Balance
Rich	0	1	2.5	0.45	6	7	0	1	Balance

Following this initial NO_X cycling test, the catalyst was loaded/poisoned with approximately 1.5 grams of sulphur per litre of catalyst. This was accomplished by passing a gas stream with a known flow rate and SO_2 concentration, as described in Table 3.2, continuously over the catalyst for 12.04 minutes. The outlet concentration of SO_2 from the reactor was recorded continuously

throughout the sulphur poisoning. With the data from the loading, which included both the sulphur inlet and outlet SO_2 concentrations, total flow rate and sulphur exposure time, the amount of sulphur deposited on the catalyst was calculated using a material balance.

Another NO_X cycling test was then conducted in order to determine the degree of catalyst deactivation. Following this second NO_X cycling test, the reactor temperature was ramped to the desired desulphation temperature in an inert gas stream containing CO_2, O_2, H_2O, He and N_2 with the same compositions listed in Table 3.2, again replacing the SO_2 flow with N_2. The desulphation experiments were then run.

After performing the desulphation, the catalyst temperature was cooled to 350^oC in the gas stream composition shown in Table 3.2 with no sulphur before another NO_X cycling test was conducted to determine the effect of the desulphation on restoring NO_X performance. Following this third NO_X cycling test, the reactor temperature was increased to 700^oC in a stream of 1% H_2, 6% CO_2, 7% H_2O and 86% N_2, and left at 700°C for 15 minutes to remove any sulphur still adsorbed to the catalyst.

3.4 Continuously Rich Flow Desulphation

For the continuously rich-phase desulphation experiments, the reactor was heated to 600^oC and the catalyst was exposed to the desulphation gas mixture for 12 minutes. The sulphur released during each experiment was calculated for comparison. Continuously rich 0.515 L/min flow and

20.84 L/min flow desulphation experiments were conducted using the gas compositions specified in Table 3.4.

Table 3.4 Continuous Flow Desulphation Gas Compositions

Run	Gas Flow [L/min]	H_2 [%]	CO [%]	C_3H_6 [%]	CO_2 [%]	H_2O [%]	O_2 [%]	He [%]	N_2
Low 1	0.515	11.8	17.8	0	8	10	0	4	Balance
Low 2	0.515	11.8	0	0	8	10	0	4	Balance
Low 3	0.515	11.8	0	0	0	10	0	4	Balance
Low 4	0.515	0	17.8	0	8	0	0	4	Balance
High 1	20.84	1	2.5	0.45	6	7	0	1	Balance

3.5 High Flow Cycling Desulphation

High flow desulphation cycling experiments were conducted at 20.84 L/min, which corresponded to a space velocity of 55000 hr^{-1}. These experiments included 3 different gas mixtures. The composition of each gas stream is outlined in Table 3.5.

Table 3.5 High Flow Desulphation Gas Compositions

Gas Stream	H_2 [%]	CO [%]	C_3H_6 [%]	CO_2 [%]	H_2O [%]	O_2 [%]	He [%]	N_2
Lean	0	0	0	6	7	10	1	Balance
Rich	1	2.5	0.45	6	7	0	1	Balance
Inert	0	0	0	6	7	0	1	Balance

During the high flow desulphation cycling experiments, the lean time was 5 seconds and the rich phase time was 20 seconds. A 25 second inert phase was imposed between each of the lean/rich gas streams during cycling to prevent mixing between lean phase O_2 and rich phase reductant.

Valve switching was initiated using an automated Labview control system. 29 cycles were used for these high flow desulphation experiments, resulting in a 12-minute combined lean/rich time. Overall, the sequence of each cycle was: 5 seconds lean → 25 seconds inert → 20 seconds rich → 25 seconds inert → repeat.

3.6 Low Flow Cycling Desulphation

Low flow cycling desulphation experiments were conducted at 0.515 L/min, which corresponded to a space velocity of 1359 hr^{-1}. Again 3 different gas mixtures were used. The composition of each gas stream is outlined in Table 3.6.

Table 3.6 Low Flow Desulphation Gas Compositions

Gas Stream	H_2 [%]	CO [%]	C_3H_6 [%]	CO_2 [%]	H_2O [%]	O_2 [%]	He [%]	N_2
Lean	0	0	0	8	10	14	4	Balance
Rich	11.8	17.8	0	8	10	0	4	Balance
Inert	0	0	0	8	10	0	4	Balance

For these experiments, the lean time was 90 seconds and the rich time was 20 seconds. The time for OSC saturation was determined from preliminary experiments. These experiments showed that under the conditions listed in Table 3.6, O_2 breakthrough during a lean phase was observed after 90 seconds. This ensured that the OSC of the catalyst sample was mostly filled prior to switching to the rich phase, which is close to 2-leg systems in practice. Again, in order to prevent reductant mixing with the O_2 at the interface between the lean and rich phases, an 80-second inert phase was employed between each of the lean/rich gas streams. Valve switching

was actuated manually and timed using a stop watch. Low flow desulphation experiments were also cycled 29 times, resulting in a 53-minute combined lean/rich time. The low flow cycle sequence followed: 90 seconds lean → 80 seconds inert → 20 seconds rich → 80 seconds inert → repeat.

CHAPTER 4: DESULPHATION ANALYSIS

4.1 Gas Composition Effects

The effect of desulphation gas composition on the extent of catalyst desulphation is discussed in this section. Although in many cases it is difficult to control the exact composition of reductant gases in vehicle exhaust, it is possible to "tune" the exhaust to have different component concentrations. Consequently, it is important to understand how different gas combinations affect the stability of sulphates on the catalyst. When formulating an effective desulphation gas mixture, this knowledge can be applied to provide the highest rate of sulphur removal from the catalyst. Although constant regenerative gas exposure is an uncommon desulphation technique compared to lean/rich cycling, due to the increased fuel penalty and lack of heat generation, the technique is useful for investigating specific aspects of desulphation, such as gas compositional effects. As outlined in the previous chapter, sulphur regeneration experiments were conducted by continuously exposing the sulphated catalyst to different gas compositions for 12 minutes at 600^{o}C. Experiments were performed both under high flow conditions and low flow conditions. In this section, the method and sequence in which sulphates were decomposed/reduced is first discussed. Following the sulphur removal analysis, the NO_X conversion performance of the catalyst before and after desulphation experiments is evaluated.

NxtGen Emission Controls Inc. did not disclose the details of their catalysts composition. For the purpose of this discussion the catalyst storage material was assumed to be Ba and the

precious metals were assumed to be Pt. Both Ba and Pt are very common components in NSR catalysts.

During continuously rich desulphation experiments, sulphur was released primarily as H_2S (Figure 4.1). It was produced during all experiments except for the desulphation experiment containing only CO_2 and CO. SO_2 was also produced during all runs except for the experiment with only CO_2 and CO (Figure 4.2). COS was produced when testing with the standard desulphation mixture, which contained H_2O, CO_2, H_2 and CO, and the desulphation mixture containing H_2O, CO_2 and H_2 (Figure 4.3). It is important to note that the absolute values for COS are not presented, due to the lack of an accurate calibration gas to quantify COS concentration. Thus, no labels are included on the y-axis of Figure 4.3. Based on the mass balances, the contribution from SO_2 and COS to the overall amount of sulphur release was much less than that of H_2S.

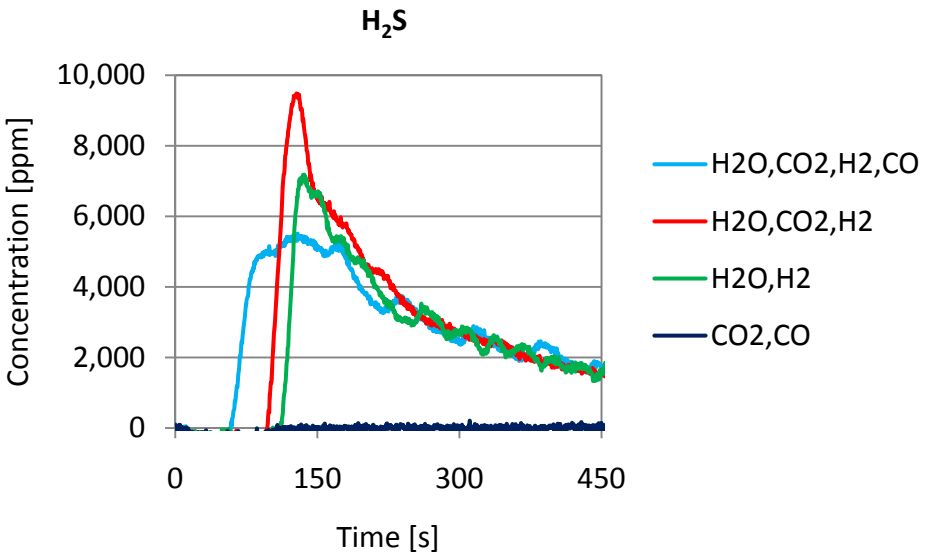

Figure 4.1 H_2S Concentration During Continuously Rich Low Flow Desulphations

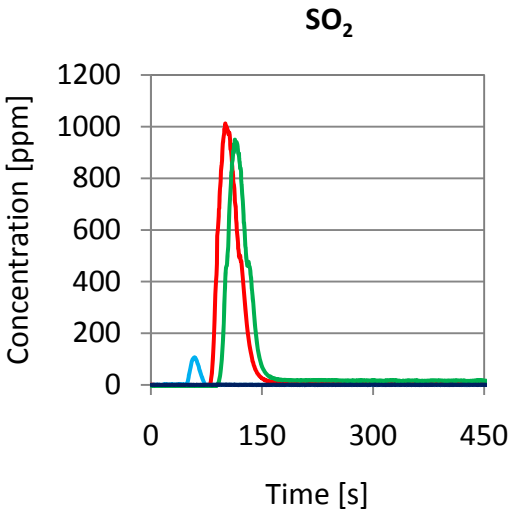

Figure 4.2 Continuously Rich Low Flow SO_2 Concentrations

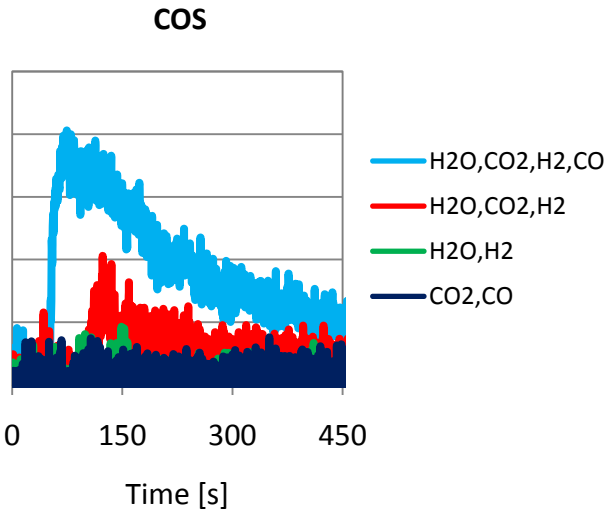

Figure 4.3 Continuously Rich Low Flow COS Concentrations

The initiation of each desulphation experiment at the start of catalyst exposure to reductant gases appears at t = 0 seconds on the x-axis of Figures 4.1, 4.2 and 4.3. The delay in observed sulphur release was due to competition between catalyst surface oxygen and the sulphate species for reaction with the entering H_2 and CO. The reaction between H_2 or CO with the surface oxygen was much faster than the reaction with sulphate species at these temperatures. Therefore, the reductants react with the surface oxygen species first, only then does the sulphate reduction begin. For the standard desulphation gas, which included both H_2 and CO, sulphur release from the catalyst was observed 20 seconds earlier compared to experiments with only H_2. The shorter delay with both CO and H_2 added was simply due to more reductant being available to react with the surface oxygen and therefore consumed it sooner. As shown in Figures 4.4 and 4.5, increased CO_2 and H_2O concentrations were observed at the start of the continuous desulphation procedure, due to CO and H_2 oxidation by surface oxygen. As CO_2 and H_2O levels decreased to the inlet concentrations, the production of sulphur products increased, representing the transition

from OSC consumption to sulphate reduction. This phenomenon is better portrayed in Figure 4.6, where initial SO_2 and H_2S production is overlayed with H_2O, CO_2, H_2 and CO concentrations for the standard desulphation mixture experiment.

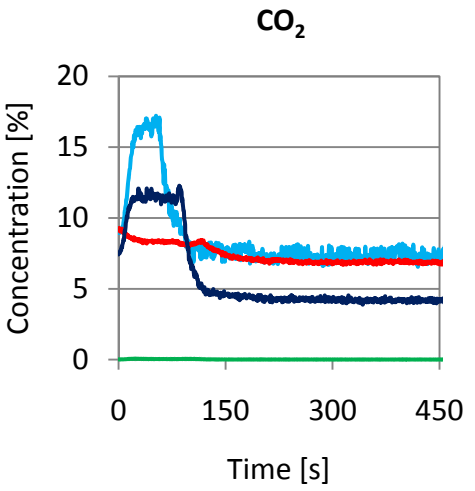

Figure 4.4 Continuously Rich Low Flow CO_2 Concentrations

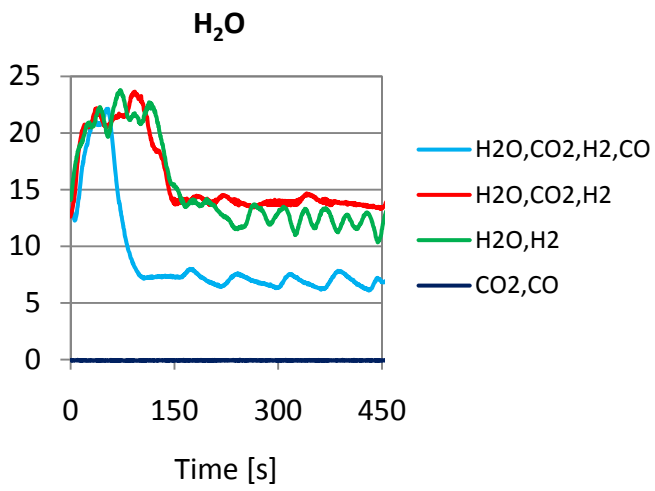

Figure 4.5 Continuously Rich Low Flow H_2O Concentrations

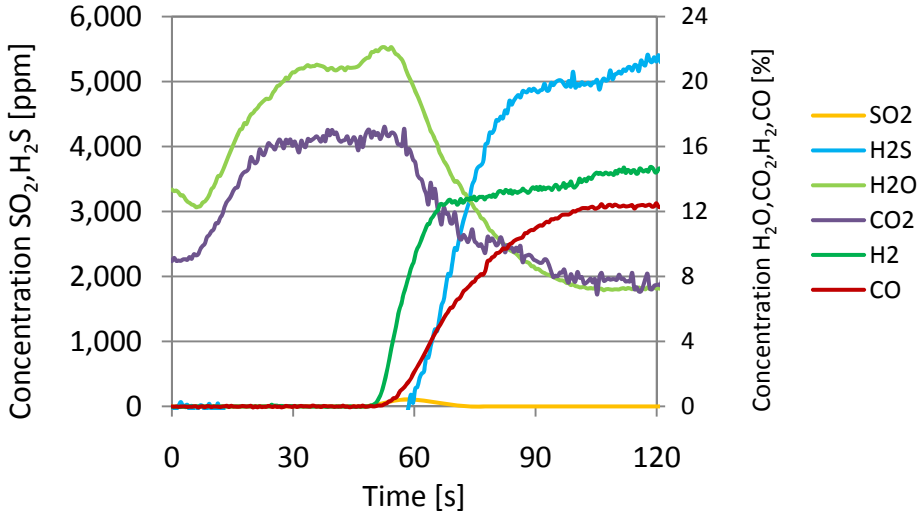

Figure 4.6 Continuously Rich Low Flow H_2O, CO_2, H_2 and CO Desulphation

The different sulphur products were released in series during desulphation. With the standard gas mixture, SO_2 was produced 60 seconds after the desulphation was initiated, and 80 seconds after the gas mixtures without CO_2, CO or both. For the standard desulphation, the SO_2 product concentration increased for approximately 10 seconds, reaching a maximum value of 104 ppm and then decreased. SO_2 concentration increases were more prolonged and a peak was achieved after approximately 20 seconds when the reductant gas mixtures were H_2O, CO_2, H_2 and H_2O, H_2. Furthermore, the maximum value of SO_2 for these latter cases was much higher than that observed with the standard gas mixture, reaching approximately 980 ppm. These data suggest that SO_2 was the sulphate decomposition product during the transition from OSC reduction reactions to sulphate reduction reactions. Following the "pulse" of SO_2, H_2S was released throughout the remaining 12 minutes of desulphation. When COS was released, it followed the same trends as the H_2S.

The release of sulphur products in series was an indicator of how the sulphates were reduced or reductants were being used. As the amount of surface oxygen decreased, through combustion with reductants, there was an increased availability of reductant for reaction with surface sulphate species. During the transition from reductant reacting with OSC to sulphate species, SO_2 production began (Equations 4.1 and 4.2). This therefore suggests that during this transition, the concentration of reductant was not great enough to drive the full reduction of catalyst sulphates to H_2S (Equation 4.3) or COS (Equation 4.4). Once all of, or at least more of, the surface oxygen was removed, reductant concentrations were locally high enough such that sulphates were fully reduced to H_2S or COS. To reiterate, Equations 4.1 to 4.4 represent reactions from Ba, the assumed storage component on the NxtGen Catalyst.

$$BaSO_4 + H_2 \rightarrow Ba(OH)_2 + SO_2 \quad (4.1)$$

$$BaSO_4 + H_2 + CO_2 \rightarrow BaCO_3 + SO_2 + H_2O \quad (4.2)$$

$$SO_2 + H_2 \rightarrow H_2S + O_2 \quad (4.3)$$

$$SO_2 + CO \rightarrow COS + O_2 \quad (4.4)$$

Equations 4.1 and 4.2 include H_2 as the active reductant in the reaction with barium sulphates. CO is not listed as a direct reductant since the results of the desulphation experiment conducted where only CO_2 and CO were present showed that no sulphur was removed from the catalyst over the course of the 12 minute desulphation (Table 4.1). This demonstrates that CO, although it may have reduced sulphates to less oxidized species, did not result in sulphur release. As shown in Equation 4.4, CO was required in order to reduce SO_2 to COS. In the experiment containing only H_2O and H_2, COS did not form since CO was not included in the desulphation gas mixture, nor could it be produced via the water gas shift (WGS) reaction.

Table 4.1 Percentage of Sulphur Removed from Continuously Rich Low Flow Desulphations

Desulphation	**Sulphur Removed [%]**
H_2O, CO_2, H_2, CO	60.39
H_2O, CO_2, H_2	60.32
H_2O, H_2	52.52
CO_2, CO	0.00

As discussed in the literature, sulphates are reduced most effectively using H_2[32,55,57]. This is confirmed by the data presented above suggesting that CO was ineffective in causing sulphur release. However, at 600°C the WGS reaction can occur very easily over catalyst Pt sites[18]. For

the case of the standard desulphation gas mixture, the H_2 concentration reached 15% which was approximately 3% higher than the inlet concentration (Figure 4.7). In the same experiment, the concentration of CO decreased by approximately 4% (Figure 4.8). At least 3% of the decrease in CO could have accounted for the increase in H_2 via the WGS reaction. The formation of H_2 via the WGS was partly driven by the decreasing concentration of H_2 as it reacted with sulphates, which in turn increased the rate of sulphur removal.

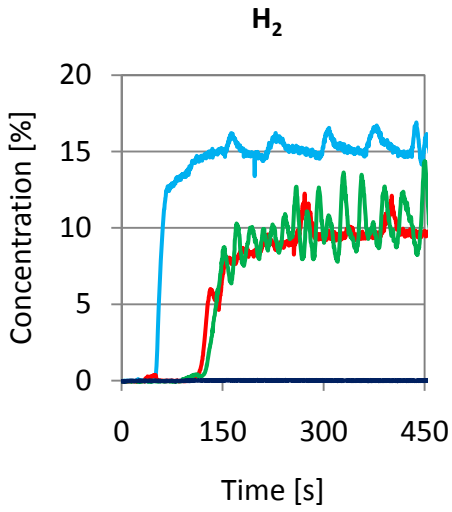

Figure 4.7 Continously Rich Low Flow H_2 Concentrations

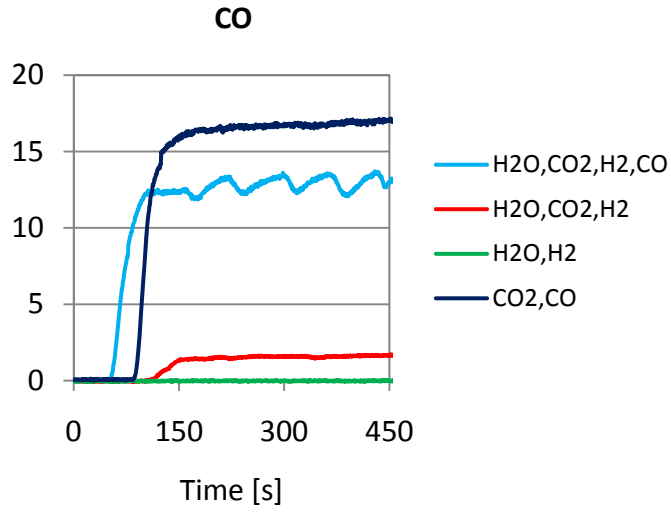

Figure 4.8 Continously Rich Low Flow CO Concentrations

Another continuously rich desulphation experiment was performed at 600°C, but under high flow conditions with C_3H_6 included in the feed-stream. Although lower concentrations of reductants were used for the high flow desulphation experiment, the amount of total reductant delivered to the catalyst was much larger due to the higher volumetric flow rate. Thus, 1 second of flow under the high flow desulphation conditions was equivalent to 10.3 seconds of flow under the standard low flow desulphation conditions, in terms of the quantity of total reductant delivered.

Due to this high delivery of total reductant, only a slight delay of approximately 1 second, for the reduction of sulphates, occurred as a result of reactions with catalyst surface oxygen (Figure 4.9). Both H_2O and CO_2 outlet concentrations reached a sharp peak at the onset of the desulphation, indicating the combustion of catalyst surface oxygen with reductants. The same initial pulse of SO_2 was produced in the high flow desulphation experiment. Although not shown in Figure 4.9, a small amount of COS was produced in the first few seconds of the high flow experiment, but did not continue to be produced over the remainder of the desulphation. This reduced quantity of COS suggests that there was a much higher selectivity for the production of H_2S under high flow conditions. The continuous high flow desulphation removed approximately 91% of the sulphur on the catalyst over 12 minutes, which was considerably larger than the percentage released by the low flow experiments. This additional sulphur removal was be attributed to the increased amount of reductant delivered to the catalyst over the course of the desulphation, as well as the overall lower sulphur product concentrations, which decreased the resistance of sulphur release due to solid/gas equilibrium limitations.

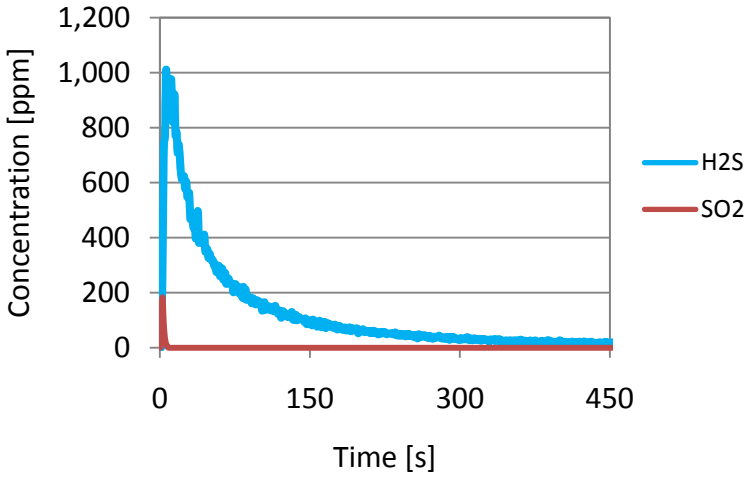

Figure 4.9 Continuous High Flow Desulphation H_2S and SO_2 Concentrations

NO_X cycling experiments were used as an indicator for the extent of sulphur removal. The NO_X storage ability of the catalyst was compared before and after exposing the catalyst to sulphur, labelled "Unpoisoned" and "Poisoned" in Figure 4.10 respectively. Additionally, the NO_X storage ability of the catalyst was compared after each catalyst desulphation in Figure 4.10. Note that the NO_X spike observed after 30 seconds, as a result of initial nitrate decomposition in the rich phase, has been cut-off to highlight the lean phase NO_X slip.

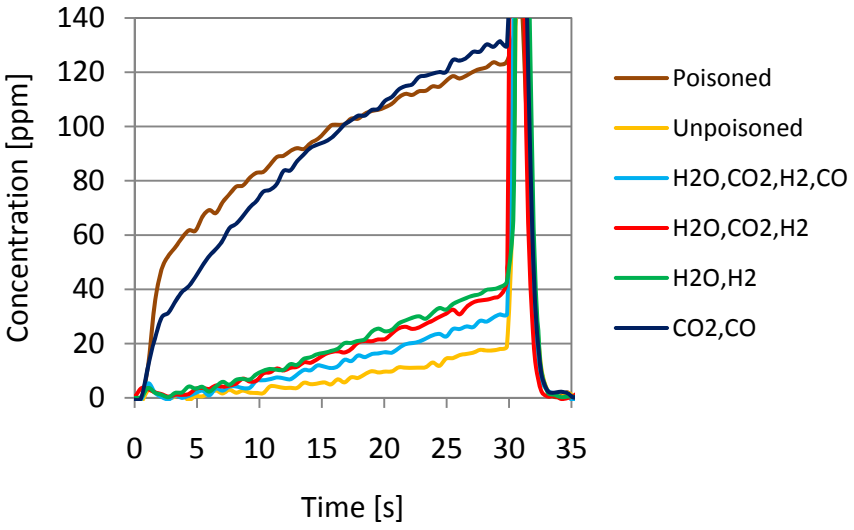

Figure 4.10 NO_X Performance After the Continuously Rich Low Flow Desulphation Experiments

As the concentration of sulphur decreased on the catalyst, it was intuitive that the NO_X slip should decrease; the lower the NO_X slip the higher the amount of sulphur removed. The standard desulphation gas mixture, which included CO_2, H_2O, H_2 and CO, resulted in the lowest loss of catalyst NO_X trapping ability. The NO_X slip was slightly worse after the desulphation with the gas mixture that contained only CO_2, H_2O and H_2. Interestingly however, there was only a small difference in the amount of sulphur removed from the catalyst between these two experiments

(Table 4.1). This difference in NO_X conversion, but similarity in sulphur removed, may be a result of the experimental error in the experiments, although this was not quantified. If the accuracy is assumed correct, it can be explained through analysis of how sulphur was removed from the catalyst. Sulphur deposition occurs on all metals and components of the catalyst, first at the front of the catalyst and then progressing downstream through the catalyst monolith[51]. Desulphation will follow a similar pattern with the front of the catalyst being regenerated first. The reduced NO_X slip with the standard mixture could be attributed to more sulphur removed from the front of the sample leading to better trapping at the front and therefore higher residence times of released NO_X during the rich phase. It is also possible that with the standard mixture, sulphur was removed from sites that are more efficient for trapping NO_X, and with more of these sites "cleaned" lower NO_X slip was attained.

When CO_2 was also removed from the desulphation gas mixture, leaving only H_2O and H_2, the subsequent recovery of NO_X performance was less effective than the first two experiments. Since CO_2 was the only gas removed, the result suggests CO_2 had an affect on the surface stability of sulphates[55]. Likely, when CO_2 was present, sulphates could be replaced with carbonate species (Equation 4.2) as well as, or instead of, hydroxide complexes (Equation 4.1), thus destabilizing the sulphate when present.

The final desulphation mixture tested contained only CO_2, CO and N_2 and it resulted in the poorest subsequent NO_X performance. Since the WGS reaction was not possible with this mixture no H_2, which was key for sulphur release, was produced. Although no sulphur was removed from the catalyst during this experiment (Table 4.1) and the total amount of NO_X

trapped (1.7 cm^3) during the NO_X tests were the same, the NO_X slip profile changed during the lean phase of NO_X cycle testing. Compared to the poisoned catalyst the initial NO_X slip profile after desulphation with only CO_2 and CO was less steep. This slight change in the trapping profile suggests that CO caused a re-distribution of sulphate species on the catalyst surface, such that either some sulphates were moved from the front of the catalyst to the rear, or from Ba sites with different efficiencies toward trapping. Alternatively, the slight change in NO_X slip may be a result of the experimental error, again this was not quantified through a statistical analysis.

CO does not directly contribute to sulphur release. The inclusion of CO in the desulphation gas stream serves to create additional H_2, via the WGS reaction, which in turn induces sulphur release. CO was responsible for the full conversion of SO_2 to COS in desulphation experiments where H_2 was present to reduce surface sulphates. H_2 was an effective reductant for both the surface sulphate reduction to SO_2 and the full reduction of SO_2 to H_2S on the NxtGen catalyst. Although only proven in one experiment, CO_2 was shown to reduce the stability of sulphates on the catalyst. The inclusion of H_2O was shown to increase desulphation effectiveness either via the production of H_2 by the WGS reaction or the prevention of BaS accumulation on the catalyst[27,54,55]. Overall, the continuously high flow rich desulphation experiment removed more sulphur than the low flow tests. An added benefit of the high flow desulphation was that sulphur products were released at much lower concentrations. This would be an important consideration when certain emission concentrations are regulated.

4.2 High Flow Cycling Desulphation Effects

Automotive lean-burn desulphation procedures use lean/rich cycling instead of a continuously rich gas exposure due to the high fuel penalty associated with prolonged periods of reductant gas generation and the benefit in heat generation associated with lean/rich cycling. High exhaust flow rate lean/rich cycling desulphations are typical for single-leg/exhaust pipe NSR automotive applications. Experiments were conducted on the NxtGen catalyst to determine how effective a standard high-flow desulphation method was in terms of subsequent catalyst performance and sulphur removal, and to compare a simulated 2-leg operation to these data, which is described in the next section. To do so, the NO_X conversion performance was determined both before and after the desulphation procedure and the amount and types of sulphur removed was measured.

The PFR had a significant length of tubing that extended between the 4-way switching valve, where alternating lean and rich phases were introduced, and the catalyst sample. As a result of this extended length, the potential for a large amount of mixing between lean and rich phases exists. The extent of inter-phase mixing that occurred through this length of tubing is not typical for single-leg or dual-leg vehicle systems. To reduce phase mixing, inert phases were used between lean and rich phases. This also allowed for a better comparison between low and high flow experiments as the two would otherwise undergo different mixing phenomena. The lean, inert and rich phase times for high flow experiments were 5, 25 and 20 seconds, respectively.

High flow cycling desulphation produced SO_2 and H_2S. The amount of COS produced during these experiments was not measureable. Figure 4.11 shows the H_2S release for the first cycle of desulphation at the four temperatures investigated.

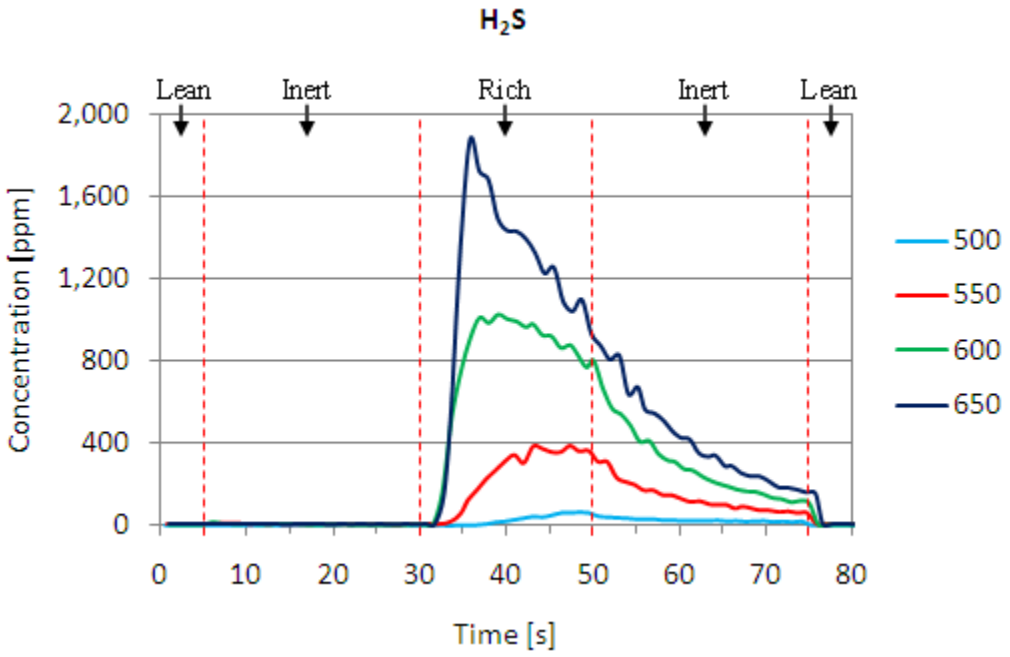

Figure 4.11 H_2S Release During the First Cycle of High Flow Desulphation Cycling

The dashed lines on the plot designate the transition between lean, rich and inert phases. The first five seconds of the plot correspond to the first lean phase of the desulphation experiment. Since no reductant was present during the lean phase, H_2S was not released during this period. The first 25-second inert phase follows the lean phase and again no sulphur products were observed during this phase since reductants had yet to be included. At the 30-second mark of the cycle, the rich phase was initiated. There was a slight delay from when reductants were introduced to the point where sulphate decomposition products were observed. This was explained by the initial combustion of reductants with catalyst OSC as was discussed in the

previous section. After the delay, a sharp rise in H_2S production was observed. The concentration of H_2S was highest at 650°C and decreased with each drop in desulphation temperature, as expected since sulphate stability decreases with temperature[53,54,55]. Following the 30-second rich phase and 25-second subsequent inert phase, another lean phase began and H_2S production ceased. Interestingly, H_2S continued to be produced during the inert phase where no reductants were available. There are several possible explanations for this continued sulphur release. First, sulphur compounds tend to be very "sticky" on metals. Sulphate products may have physisorbed to the walls of the downstream stainless steel tubing during the rich phase, between the catalyst and analyzer. After the transition to the inert phase, this physisorbed sulphur could desorb due to the change in concentration gradient between the reactor walls and the gas-phase, resulting in the continued release through the inert phase. Second, sulphate reduction products may have chemisorbed to catalyst components after their release. During the inert phase, these products again could desorb due to the change in concentration gradient. It is uncertain which of these mechanisms was responsible for the continued production of sulphate reaction products during the inert phase.

The production of SO_2 followed similar trends as H_2S production. One difference was that much lower concentrations were produced, with peak concentrations ranging between 35 ppm at 500°C and 515 ppm at 650°C. Interestingly, during the second lean phase of the cycle, a sharp spike in the SO_2 release was observed (Figure 4.12). The precious metal sites can be poisoned by sulphur originating from the Ba components during the rich phase, forming Pt-S[49]. The subsequent introduction of O_2 would oxidize the sulphur from precious metal sites producing SO_2. The length of time that SO_2 was produced during the actual rich phase of cycling decreased with

increasing desulphation temperature and at 600°C and 650°C the release of SO_2 was limited to the first half of the rich phase. Since at both of these higher temperatures, higher H_2S concentrations during the rich phase were observed, the decreased time that SO_2 was produced suggests a quicker transition in reaction mechanism. Several simultaneous reactions are occurring. The first reaction is of course sulphate reduction, but also as temperature increased the reduction of any released SO_2 to H_2S would occur at higher rates in the presence of reductants. As discussed in the previous section, reductants and surface oxygen react at the onset of the rich period. The reaction interface between OSC and sulphate reactions was where SO_2 was produced. Since the rate of reductant delivery to the catalyst was the same for all experiments and SO_2 release time decreased with increasing temperature, the data suggests that at higher temperatures the selectivity of OSC and sulphate reactions was influenced. Another possibility is that at higher temperatures the rate of OSC consumption, or the SO_2 to H_2S reaction, was no longer kinetically limited. This overall change in selectivity is an important aspect of desulphation, especially because H_2S is harmful to human health and the associated odour is unacceptable. Additional catalyst metals or exhaust-treatment technologies may be required if high H_2S concentrations are produced, thereby increasing costs[62].

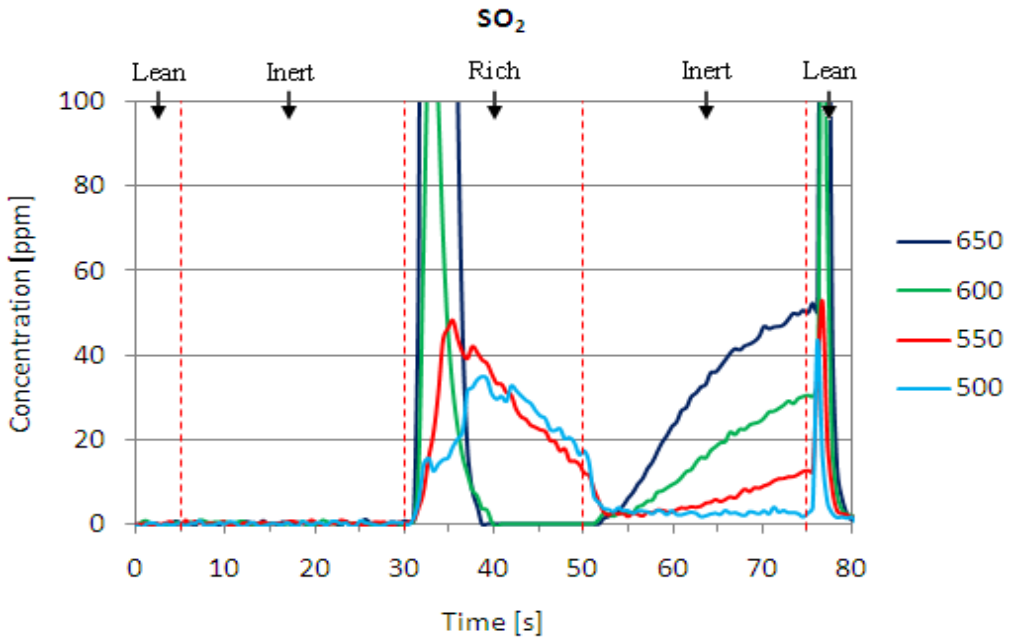

Figure 4.12 SO_2 Release During the First Cycle of High Flow Desulphation Cycling

Each of these experiments was performed for 29 cycles. The peak concentration of sulphur within each cycle decreased over the course of the experiment, as shown in Figure 4.13 for H_2S. The peak concentration of H_2S at the end of experiments ranged between 4 ppm at 650°C and 20 ppm at 500°C. The reason for the higher 500°C H_2S concentration at the end of cycling, compared to the 650°C experiment, is that far more sulphur remaining on the catalyst, 8% at 650°C compared to 84% at 500°C, thus peak concentrations were slightly higher.

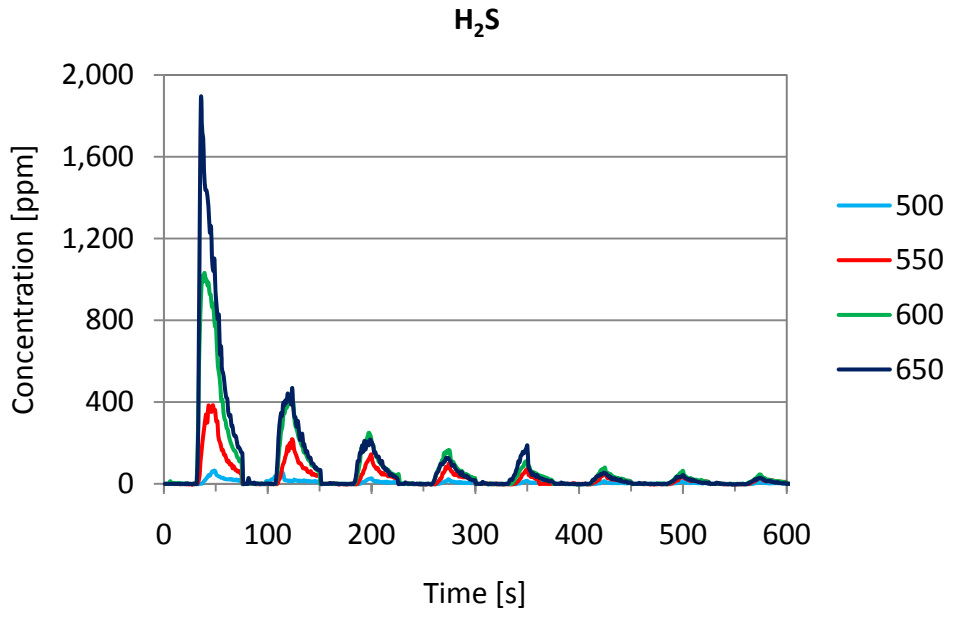

Figure 4.13 High Flow Cycling H_2S Release Over Eight Cycles of Desulphation

The total volume of cycle-by-cycle sulphur release is shown in Figure 4.14. Prior to each desulphation experiment, approximately 23.5 cm^3 of sulphur was deposited on the catalyst. At 650°C, just over 50% of the sulphur stored on the catalyst was released in the first cycle. As the desulphation temperature was decreased, less total sulphur was released during the first cycle; 35% for 600°C, 13% for 550°C and 2% for 500°C. At the higher temperatures, the first few cycles of desulphation removed the bulk of sulphur from the catalyst. At 600°C and 650°C, there was a dramatic decrease in the amount of sulphur release after the first few cycles. For example, at 650°C, the first cycle released 11.5 cm^3 of sulphur, the second cycle released 3.6 cm^3 and the third cycle released 1.7 cm^3. At 500°C and 550°C, the decrease in sulphur release with each cycle was not as dramatic as at the higher temperatures because of the larger amounts remaining on the surface to take part in reaction during subsequent cycles.

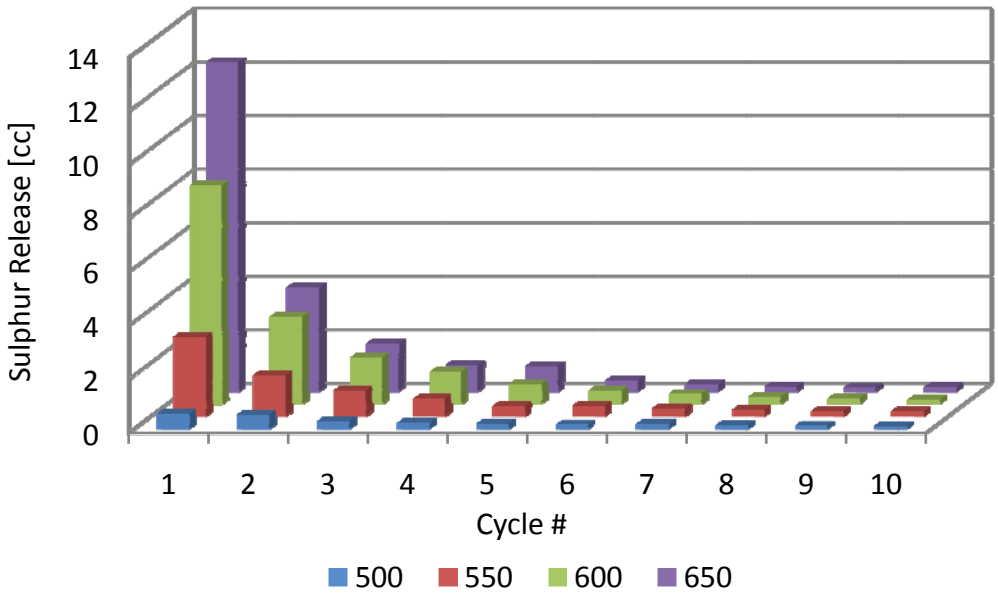

Figure 4.14 High Flow Cycling Desulphation Cycle-by-Cycle Total Sulphur Release

The data demonstrate that a very limited amount of sulphur was removed from the catalyst at 500°C and 550°C (Table 4.2). This indicates that desulphation procedures below 550°C would not be effective for the removal of sulphates under these high flow conditions. With desulphation temperatures above 550°C, the overall sulphur release increased to 75% and 91% for 600°C and 650°C, respectively.

Table 4.2 Percentage of Sulphur Removed During High Flow Desulphation Cycling

Desulphation Temperature [°C]	**Sulphur Removed [%]**
500	15.7
550	38.9
600	74.1
650	91.3

As the number of cycles in each experiment progressed, the concentration of sulphur on the catalyst decreased. Thus, less reductant was consumed in reactions with sulphates and the outlet reductant concentrations gradually increased with each cycle, as shown in Figures 4.15 and 4.16. The increase in reductant concentration was most apparent at 650°C, which removed the largest amount of sulphur in the first cycles. Lower desulphation temperatures had sequentially higher initial reductant breakthrough as a result of lower amounts of sulphur reduced with each cycle.

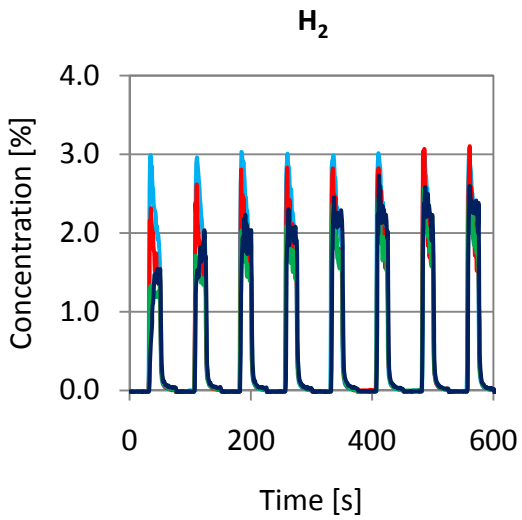

Figure 4.15 H_2 Concentrations for High Flow Cycling Desulphations

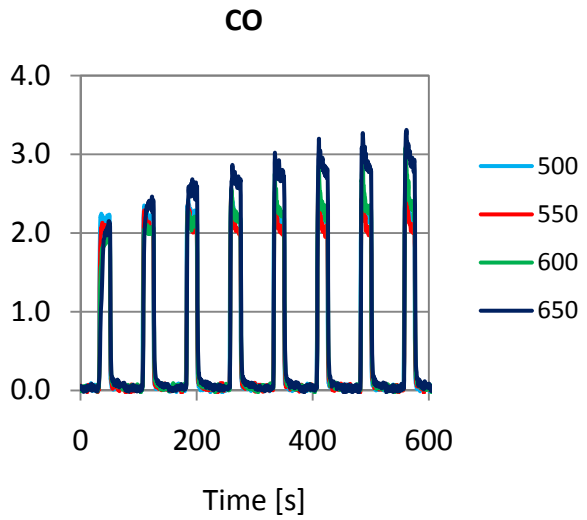

Figure 4.16 CO Concentrations for High Flow Cycling Desulphations

When steady cycle-to-cycle sulphur release was achieved during the eighteenth cycle, the concentration of reductant in the outlet gas stream also steadied. The outlet H_2 concentration at steady state cycling was approximately 2.75%. This is greater than that in the inlet by an increase of 1.75%. If this was simply due to the WGS reaction, the outlet concentration of CO would be approximately 1.75% lower than the inlet concentration. However, this was not the case since the CO concentration also increased, with the largest change occurring at 650°C, by 0.75%. The increase in H_2 and CO outlet concentrations was due to the inclusion of C_3H_6 in the

high flow reductant gas mixture. A plot of C_3H_6 concentrations (Figure 4.17) during the desulphation experiments shows decreasing outlet concentrations of C_3H_6 as the desulphation progressed to steady state. The 650°C desulphation exhibited the largest change from inlet concentration. C_3H_6 can be partially oxidized on the catalyst with the surface oxygen to produce CO, or undergo steam reforming to H_2 and CO as products[17,44]. For every C_3H_6 partially oxidized or reformed, three CO molecules could be produced. Once stable cycling was reach, the concentration of C_3H_6 for the 650°C experiment was 0.1%. This means 0.35% was converted either by oxidation or desulphation. If all C_3H_6 were converted to CO, then the CO concentration could increase by approximately 1%. However, since CO increased by 0.75%, some of the C_3H_6 was likely fully oxidized to CO_2. The CO_2, or lack of all C_3H_6 going to CO, could either be due to oxidation with the surface oxygen or the WGS reaction producing H_2. The excess H_2 produced relative to the 0.25% CO that could have been consumed in the WGS reaction, suggests that most of the H_2 originated from C_3H_6 reforming (Equation 4.5).

$$C_3H_6 + 6H_2O \rightarrow 9H_2 + 3CO_2 \quad (4.5)$$

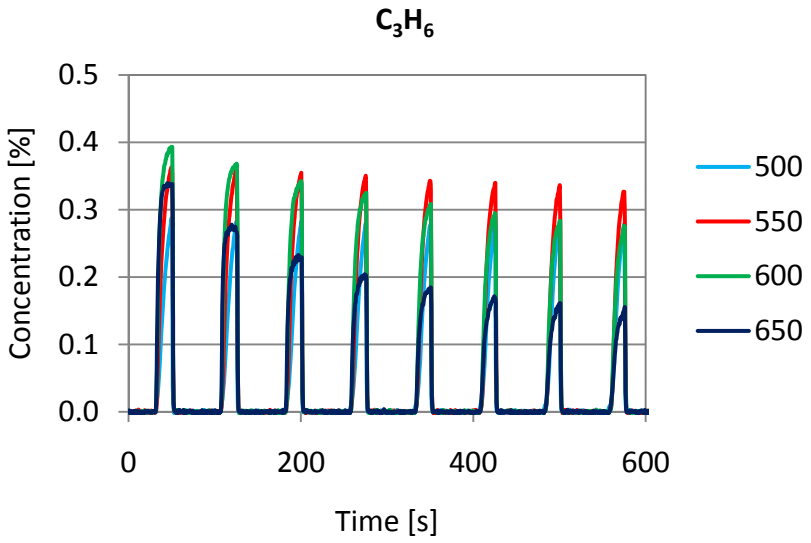

Figure 4.17 C_3H_6 Concentrations During High Flow Desulphation Cycling

An initial increase in CO_2 concentration during each rich phase of the cycle was apparent for all cycles, followed by a slight increase in concentration (Figure 4.18 shows only the first cycle). At the same time, an initial increase in H_2O concentration was observed followed by a decrease in the amount of H_2O during rich phases (Figure 4.19). The initial increase in H_2O and CO_2 was a result of reductant combustion with catalyst OSC. During each rich phase of the cycle, the amount of reductant fed to the reactor including H_2 and CO, was 262.2 cm^3 (calculated on a stoichiometric equivalent basis for reductant combustion with O_2) compared to the 25 cm^3 of catalyst oxygen at the same temperature. Since this was approximately 8 times the amount of surface oxygen on the catalyst, the effect of OSC would have only been apparent during the first two seconds of the cycle compared to the effect of the WGS and steam reforming reactions. The decrease in H_2O which follows the initial increase, and the slight increase of CO_2, are likely caused by the WGS and steam reforming reactions.

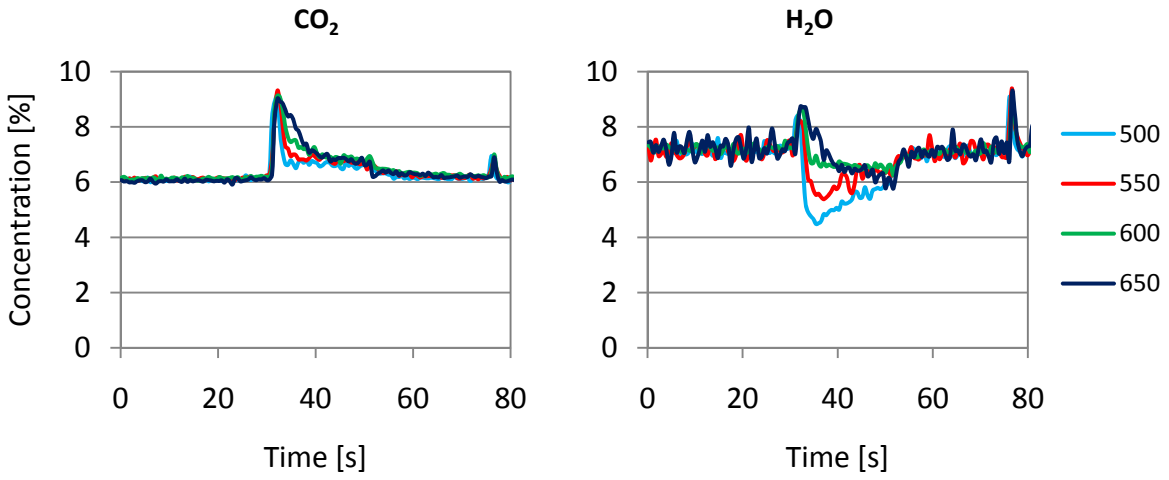

Figure 4.18 CO_2 Concentration During the First Cycle of High Flow Cycling

Figure 4.19 H_2O Concentration During the First Cycle of High Flow Cycling

The NO_X cycling performance before and after sulphur poisoning, and after the 4 desulphation experiments, is shown in Figure 4.20. These tests were performed at 350°C with 30 second lean phases and 5 second rich phases. It was apparent that the 500°C desulphation experiment resulted in the worst NO_X performance recovery. A large improvement in performance was noted after the 550°C desulphation, while the highest recovery in NO_X performance occurred at 600°C and 650°C. Although more sulphur was removed from the catalyst at 650°C than 600°C, the two experiments had similar NO_X slips. The presence of multiple sulphur stabilities on the catalyst explained this trend, as was discussed in the previous section. Less stable sulphates would have been first removed from the catalyst during desulphation, while more stable sulphates would remain on the catalyst until higher temperatures are used. Since there was no difference in NO_X performance after the two higher temperature experiments, the majority of NO_X storage likely occurred on catalyst sites where lower stability sulphates were removed. It was assumed that if longer lean periods during the NO_X cycling experiments were investigated

for the 600°C and 650°C NO_X tests, there would be a noticeable difference in NO_X storage as a result of NO_X sorption on more stable catalyst sites.

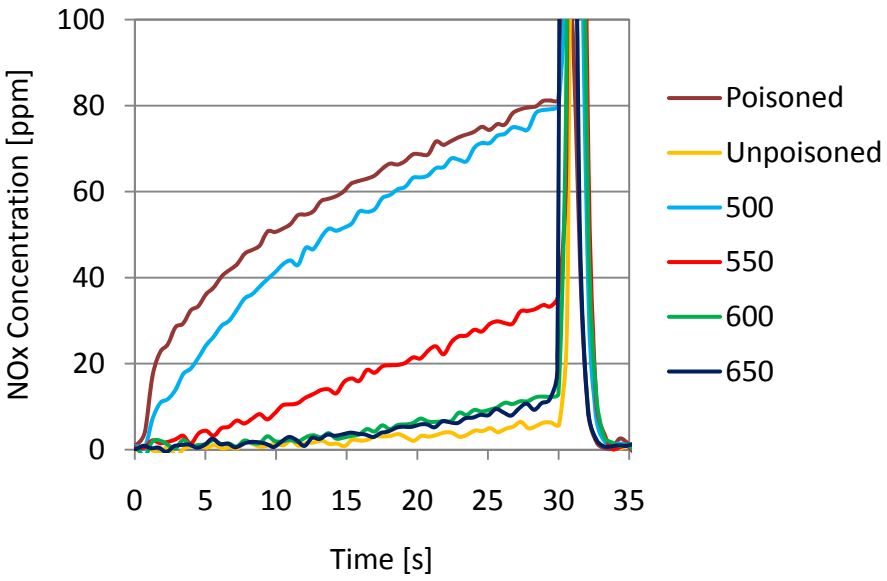

Figure 4.20 NO_X Performance Before and After Sulphur Poisoning and After Desulphation at High Flow Cycling Conditions

4.3 Low Flow Cycling Desulphation Effects

The NxtGen process was specifically designed for use in a 2-leg NSR automotive application. To effectively test the catalyst for this application, low flow cycling experiments were designed to mimic the desulphation method of a 2-leg system. In a 2-leg system, lean phases are fed under high flow conditions while rich phases are introduced under significantly lower flow conditions. Low flow conditions are desired to minimize the size of the fuel reformer and fuel penalty. In order to avoid complications associated with different mixing phenomena when testing with either the low or high flow conditions, an inert phase was imposed between the lean and rich

phases. In these low flow experiments, an inert phase of 80 seconds was used. Lean phases were maintained for 90 seconds and rich phases for 20 seconds. The lean phase was extended for much longer than in the high flow experiments to saturate the catalyst OSC by the end of each lean phase. This made the experiment and results more comparable to the high flow experiments where the catalyst OSC was always saturated after the lean phase of each cycle.

The main sulphate decomposition products during the low flow desulphation cycling experiments were SO_2 and H_2S. The concentration of SO_2 was consistently higher than that of H_2S, whereas with high flow cycling the opposite was observed. Under low flow cycling conditions, sulphur was not observed in the outlet gas until several cycles of desulphation had been completed (Figure 4.21). On the third cycle of the desulphation experiment at 650^{o}C, SO_2 was observed, but not H_2S. For the 600^{o}C and 550^{o}C experiments, SO_2 was produced during the fourth cycle, again without H_2S. No significant amount of sulphur release was observed during the 500^{o}C experiment. Beyond the first four cycles of desulphation, the concentration of SO_2 during each rich phase increased until a peak concentration of SO_2 was observed at all temperatures around the ninth cycle. The peak concentrations of SO_2 released were higher for the 600^{o}C and 650^{o}C experiments relative to the 500^{o}C and 550^{o}C experiments. For the first 11 cycles, no H_2S was produced. However, after the 11th cycle, a transition from SO_2 to H_2S as the gas-phase product was observed (Figure 4.22). In comparing the maximum release in each cycle, a peak in H_2S concentration was observed around the eighteenth cycle, which was also where SO_2 production reached a constant cycle-to-cycle release. After this peak in H_2S concentration, the peak in H_2S release in each cycle declined in a near linear fashion. At 500^{o}C, no distinguishable profile for either SO_2 or H_2S was obtained.

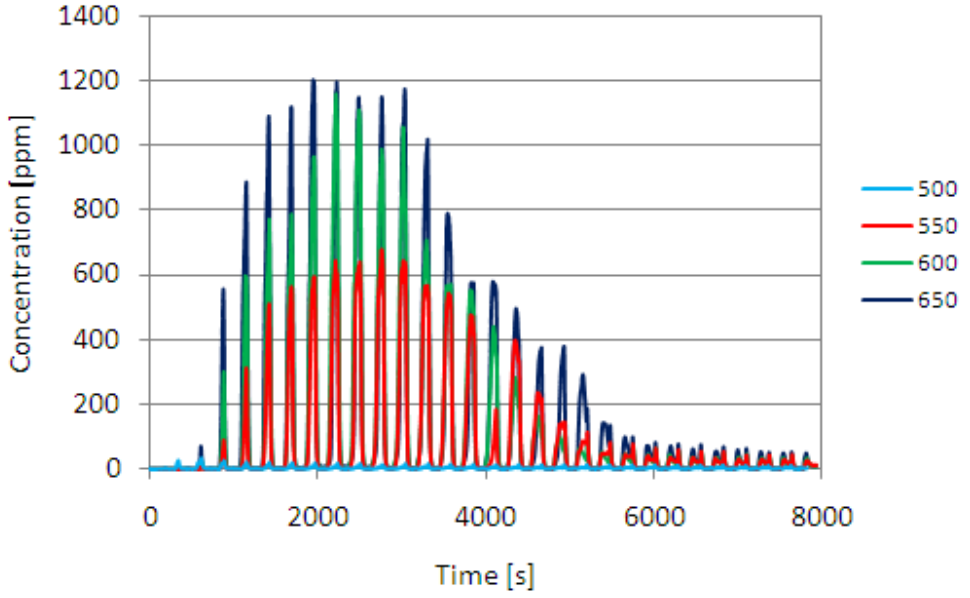

Figure 4.21 Low Flow Cycling Desulphation SO_2 Production Through 29 Cycles

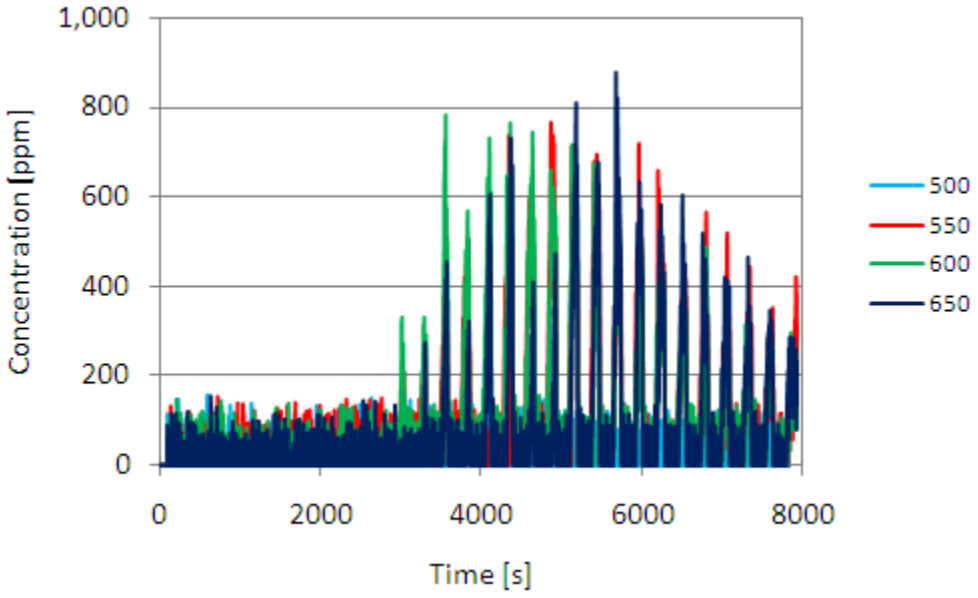

Figure 4.22 Low Flow Cycling Desulphation H_2S Production Through 29 Cycles

As was discussed previously, one of the reasons for the delay and sequence in gas-phase products associated with the release of sulphur was due to the reaction of reductant gases with stored oxygen on the catalyst. This was verified for these experiments through the analysis of outlet H_2 concentrations from the reactor (Figure 4.23). H_2 breakthrough during the rich cycles of the 500°C desulphation attained a maximum concentration of 2%. Since the inlet concentration to the reactor was 11.8%, a significant amount of H_2 was consumed by catalyst oxygen. At higher desulphation temperatures, the maximum breakthrough concentrations of H_2 were even less since some was reacting with sulphate species. The same decrease in reductant breakthrough was observed for CO, although it was more significant. A maximum outlet concentration of 0.3% CO was observed when the inlet concentration was 17.8%.

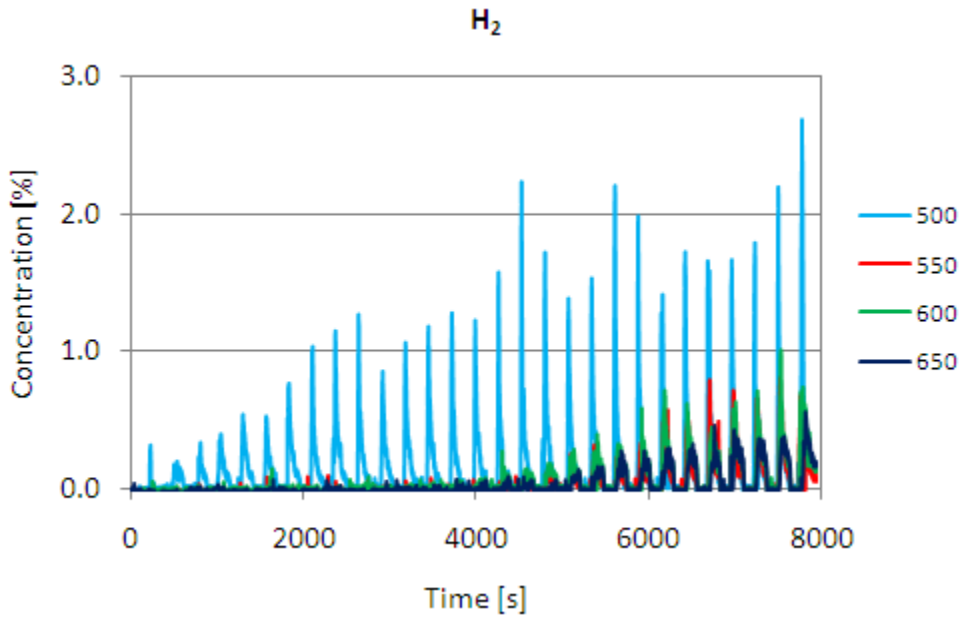

Figure 4.23 Low Flow Cycling Desulphation H_2 Concentrations Through 29 Cycles

Catalyst OSC was assumed to be saturated to the same degree during each lean phase. However, as sulphates were removed from the catalyst the amount of un-poisoned oxygen storage sites increased. If the assumption that the catalyst OSC was saturated during each lean phase was invalid, the amount of surface oxygen would have slowly decreased as cycling progressed, therefore increasing sulphate reduction. Additionally, the selectivity between reductant OSC reactions and reductant sulphate reactions would have shifted through the course of lean/rich cycling as a result of slight variations in OSC for each cycle. The change in selectivity was not solely explainable by a shift in OSC versus sulphate reactions. More intuitively, the sequential release of sulphur was either related to incompletely filling the OSC or could be explained by multiple sulphate stabilities on the catalyst. This essentially implies that less stable sulphates were decomposed during the first portion of cycling, to produce SO_2. As the concentration of low stability sulphates on the catalyst decreased, reductants began to react with more stable sulphates. The reaction with higher stability sulphates would result in the production of H_2S. The various surface stabilities of sulphates may be a result of sulphur deposition at various locations on the catalyst or could be associated with the different catalyst components. One factor might be how near the sulphate was to the precious metals on the catalyst. However, since the composition of the NxtGen catalyst is unknown, it was impossible to determine where different sulphates would be deposited or which components were poisoned and from which component the sulphur was released.

The overall amount of sulphur released from the catalyst is summarized in Table 4.3. As expected from the SO_2 and H_2S release values, the highest amount of sulphur was removed from the catalyst at 650^{o}C. With each decrease in temperature, the amount of sulphur released from

the catalyst decreased. The 500°C desulphation removed only 3% of the sulphur deposited on the catalyst. The large change in sulphur removed between 500°C and 550°C, which was approximately 40%, suggests that there was a large change in the stability of sulphates on the catalyst at temperatures above 500°C under the low flow desulphation conditions. For the low flow cycling experiments, this difference was extremely significant and can be used to define the minimum temperature of desulphation to ensure that effective catalyst regeneration is achieved.

Table 4.3 Sulphur Removal Percentages from Low Flow Cycling Desulphations

Desulphation Temperature [°C]	**Sulphur Removed [%]**
500	2.7
550	43.1
600	51.9
650	53.1

The NO_X trapping performance of the catalyst before poisoning, after poisoning and after each desulphation experiment is plotted in Figure 4.24. These tests show that there was not a significant difference between the 650°C and 600°C experiments in terms of NO_X slip. As there was little difference between the amounts of sulphur removed from each experiment, this was not surprising. The experiment at 550°C, which showed about 10% less sulphur removal compared to that at higher temperatures, also exhibited a slightly lower NO_X performance compared to the higher temperatures. Interestingly, although only 3% of the sulphur was removed from the catalyst at 500°C, the NO_X performance of the catalyst increased compared to the performance of a fully poisoned sample. This result was explained by the existence of multiple sulphate stabilities on the catalyst surface. Sulphur released from sulphates with lower stabilities was subsequently re-adsorbed further down the catalyst on more stable sites. Over the

duration of the desulphation, enough of the low stability sulphate sites on the catalyst were regenerated to permit some NO_X trapping and conversion ability. From this result, one may hypothesize that once all possible high stability sites are filled at lower temperatures, NO_X conversion would not change.

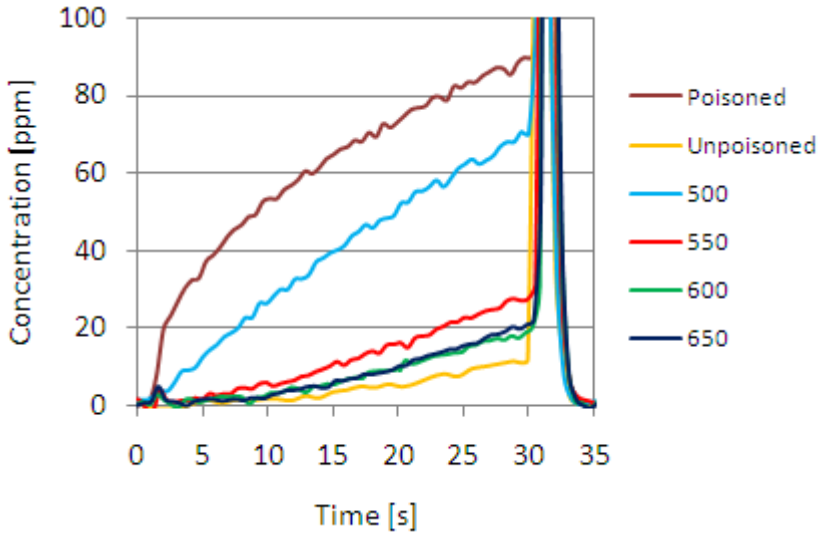

Figure 4.24 NO_X Performance Before and After Sulphur Poisoning and After Desulphation at Low Flow Cycling Conditions

To evaluate the effect of catalyst OSC on desulphation efficiency or reductant use, two additional low flow desulphation experiments were conducted at 600°C. The first experiment was designed to reduce the amount of OSC saturated during the lean phases in order to reduce the amount of reductant consumed by OSC during rich phases, and hence increase the amount of available reductant for sulphate reduction. All low flow desulphation cycling conditions remained the same for this experiment except for lean phase length which was reduced to 45 seconds, corresponding to roughly half the time required for OSC saturation. The second experiment was designed to investigate the effect of an increased rich-phase flow rate, under

otherwise the same conditions, on the ability to reduce sulphates. This experiment was conducted at a flow rate of 1.029 L/min.

The results of the desulphations, analyzed on a cycle-by-cycle basis, are shown in Figure 4.25. Comparing the first cycle of the reduced lean time desulphation experiment (0.515 45s) and the standard desulphation experiment (0.515) shows no difference in sulphur release during the first cycle. This result was expected as conditions leading to the first lean cycle, prior to the desulphation, were lean and therefore both catalysts were saturated with oxygen for the first cycle. A large difference was noted in the second and third cycles however. As a result of the decrease in lean phase time, the second cycle of the "0.515 45s" experiment had a decreased amount of oxygen on the surface which in turn increased the availability of reductant for sulphate decomposition and reduction reactions. As a quantitative example, after the first three cycles the standard desulphation released 0.1% of the stored sulphur while the reduced lean time desulphation released 16% of the stored sulphur, all due to the change in the amount of reductant consumed by stored oxygen on the catalyst. When the flow rate of the desulphation gas was doubled (1.029), the sulphur released after three cycles was 43%. A key effect of doubling the flow rate was doubling the amount of reductant introduced into the reactor. As the oxygen saturation of the catalyst was relatively unchanged between the standard flow rate and doubled flow rate, enough reductant was available with the increased flow rate to react with both the stored oxygen on the catalyst and sulphate species. This again reinforces the significant effect OSC had on efficient use of reductant gas. After 10 cycles, the shorter lean time and doubled flow rate experiments removed 55% and 64% of stored sulphur, respectively. The standard desulphation only removed 13% of stored sulphur.

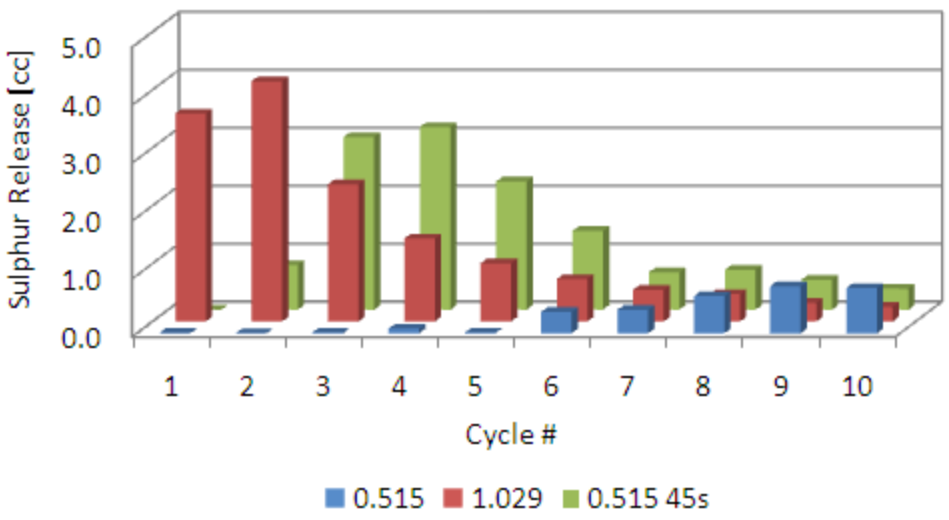

Figure 4.25 Cycle-by-Cycle Sulphur Release at 600°C for Changing Flow and Lean Phase Time

Another effect of doubling the flow and halving the lean phase time was the change in selectivity of sulphur reaction products during desulphation. Overall, of the total sulphur released in the standard 0.515 L/min desulphation experiment approximately 40% was in the form of H_2S and the remaining 60% was in the form of SO_2. It was expected that by decreasing the catalyst OSC saturation, SO_2 production would decrease with each subsequent lean phase and the amount of H_2S produced would increase. When the lean phase time was halved the percentage of sulphur released in the form of H_2S increased to 85% from 40% in the standard desulphation experiment. A further increase was observed for the doubled flow rate experiment, with H_2S accounting for approximately 93% of the total sulphur released. This result further reinforces the significance that OSC saturation has on the selectivity of sulphate reaction products.

From Figure 4.26 it was clear that doubling the flow or halving the lean phase time resulted in a more significant recovery of NO_X conversion, further reinforcing the findings of the cycle-by-

cycle sulphur analysis. Reducing the length of the lean phase increased the NO_X performance of the catalyst to a similar degree as that of doubling the flow rate. From these experiments, it was verified that at low flow rates, the desulphation of the NxtGen catalyst was dominated by OSC. To effectively apply this catalyst for a 2-leg NSR application, it would be essential to select a rich time that is long enough to consume the catalyst OSC and also provide additional reductant for sulphate reduction.

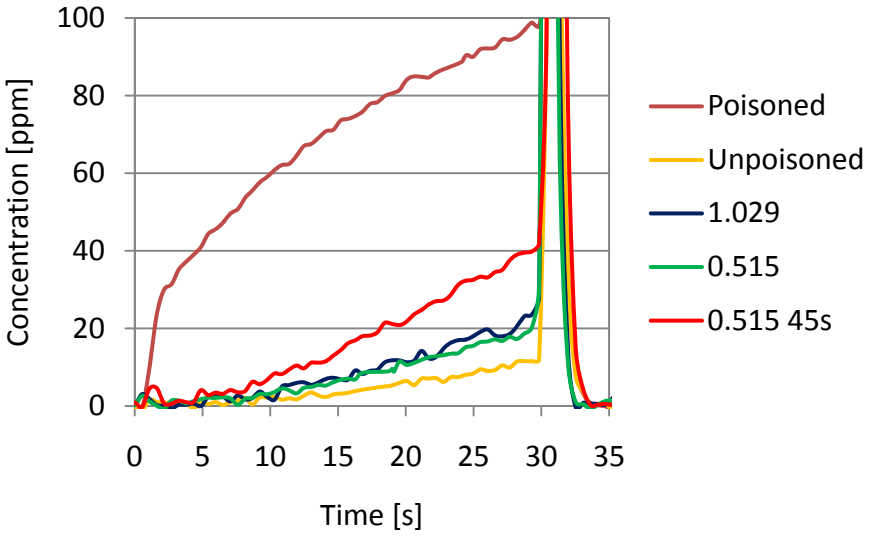

Figure 4.26 NO_X Performance at 600°C for Changing Flow and Lean Phase Time

4.4 Comparisons of Desulphation Methodology

The results demonstrated that operating conditions have a strong effect on sulphate decomposition and sulphur removal from the NSR catalyst. The data show that flow, temperature and gas compositions affected sulphur release rates and the type of species released. Three separate groups of experiments have been individually discussed: continuous regeneration

by gas exposure at 600°C, high flow cycling and low flow cycling. Each experimental set was designed so that it could be compared to each other. For cycling experiments, the combined rich time over 29 cycles totalled 9.6 minutes. Therefore, cycling experiments can be compared to 12-minute continuous rich desulphation experiments for the first 9.6 minutes of desulphation, on the basis of reductant exposure time. The results of these comparisons are discussed in this section.

A comparison of the cumulative sulphur removed at 600°C using the different desulphation methods is shown in Figure 4.27. The stored amount of sulphur on the catalyst prior to desulphation experiments is also plotted. In comparing the experiments conducted at high flow rates to those at low flow rates after the first few minutes of desulphation, the high flow conditions induced nearly 75% release of stored sulphur on the catalyst, while sulphur release only began at this same time under conditions of low flow. At the end of nine minutes of desulphation, 25% more sulphur was released using the high flow conditions relative to the amount released for the low flow conditions. Overall, the high flow desulphation conditions initially resulted in more sulphate decomposition and sulphur release compared to the low flow experiments, but if enough time was permitted the cumulative release for low flow became more comparable. A comparison of cycling experiments to the continuous 12-minute reductant gas exposure experiments (identified by "Cont" in the legend) shows that the continuous exposure to rich conditions was more effective in releasing sulphur than cycling between lean and rich for a cumulative rich time of 9 minutes. This was at least partially due to having to consume the surface oxygen repeatedly at the beginning of each rich phase portion of the cycle. However, as mentioned previously, running the diesel engine so that there is a continuous reductant-rich gas

flow is difficult due to engine operation limitations, an associated high fuel penalty and challenges in raising the catalyst temperature.

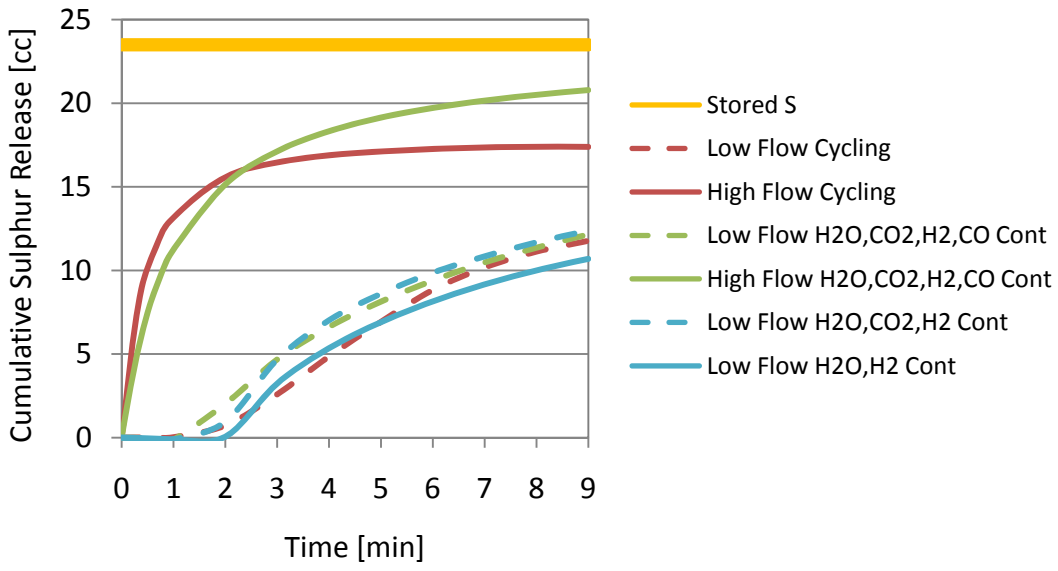

Figure 4.27 High Flow, Low Flow, Continuously Rich and Cycling Desulphation Methodology Comparison at 600°C

A cycle-by-cycle analysis of the sulphur released during high flow cycling conditions at 650°C is shown in Figure 4.28 (note the high flow H_2S data were divided by a factor of 6 for scaling purposes). The high flow conditions resulted in 91% release of the stored sulphur over the duration of the experiment while the low flow released only 53% of the stored sulphur. With the high flow conditions, the majority of sulphur was removed in the first five cycles. As a result of competition between OSC and sulphate species for the reductant, sulphur released during the low flow experiments started only after several cycles and did not drop immediately after the first evidence of release. These results show that with cycling, the most beneficial desulphation strategy for vehicle application in terms of rate of sulphur release under the conditions tested,

would be the high flow cycling desulphation method. When comparing the fuel penalty associated with either high or low flow desulphation, high flow desulphation was also more efficient. Over the course of 29 cycles at low flow conditions, the cumulative rich phase time was 580 seconds and over that time approximately 50% of the sulphur on the catalyst was removed at 600°C and 650°C. Under high flow conditions the equivalent amount of reductant was supplied to the catalyst in just 56 seconds, or less than 3 rich cycles. At the end of the third cycle approximately 77% of sulphur was removed from the catalyst during the experiments at 600°C and 650°C. The large amount of sulphur released in the first few cycles permitted much shorter desulphation durations, which in turn resulted in a lower fuel penalty and lowest potential time for thermal degradation to occur.

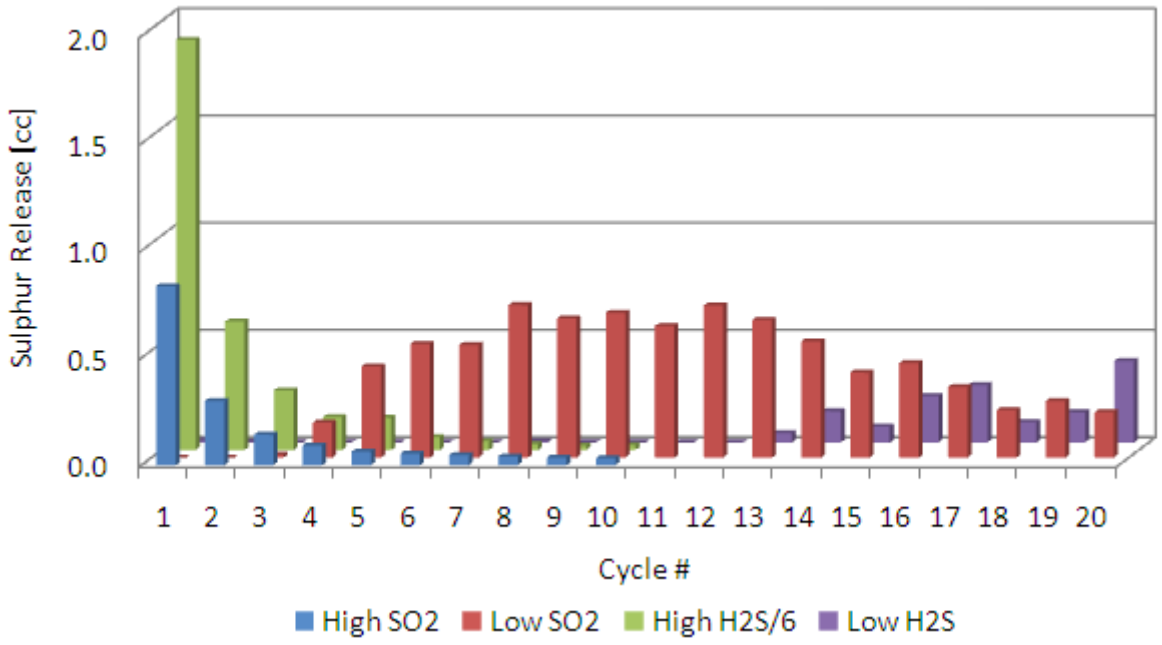

Figure 4.28 Cycle Analysis of High Flow and Low Flow 650°C Desulphation
(High Flow H_2S Data Divided by a Factor of 6 for Scaling Purposes)

Another comparison of sulphur release during high flow and low flow cycling at the various temperatures is shown in Figure 4.29. In both sets of experiments, the amount of sulphur released at 500°C was the least. Low flow cycling experiments at 550°C, 600°C and 650°C were all relatively comparable. This suggests that under low flow conditions the best temperature for sulphur removal, along with minimized thermal degradation and fuel penalty, is 550°C which is lower than the optimal temperature required for high flow conditions. Higher temperatures did not have such a significant impact and would only add to the fuel penalty and thermal degradation without an offsetting large increase in sulphur removal.

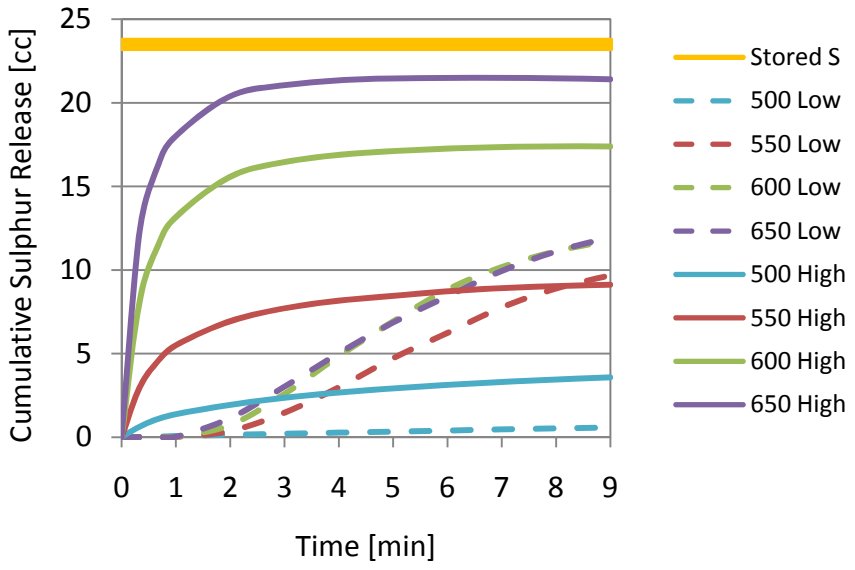

Figure 4.29 High and Low Flow Cycling Desulphation Cumulative Sulphur Released Through Nine Minutes of Combined Rich Phase Time

Results discussed in the previous section showed that some modification to the low flow conditions increased sulphate removal from the catalyst. These consisted of halving the lean phase time in one experiment and doubling the low flow rate in the other. Comparison of the

data from these experiments with the high flow cycling data indicated that both doubling the flow rate and decreasing the lean phase time increased the sulphur release from the catalyst to the extent that they were more comparable with high flow desulphation extents (Figure 4.30). Over the course of 29 cycles at the doubled low flow rate, approximately 70% of the sulphur on the catalyst was removed. In just 112 seconds, or less than 6 rich cycles, the equivalent amount of reductant was supplied to the catalyst under high flow conditions. At the end of the sixth cycle of high flow desulphation, approximately 87% of sulphur was removed from the catalyst. By simply doubling the flow rate, an improvement of 10% in the difference between high and low flow sulphur release was attainable over the standard 0.515 L/min experiment. To further optimize the low flow cycling desulphation method, the results suggested an even shorter lean period, perhaps 20 seconds lean and 20 seconds rich, combined with an increased flow rate during desulphation. This would provide for a much faster rate of sulphur release from the catalyst, which may have proved to match or even surpass the rate of sulphur release at high flow conditions.

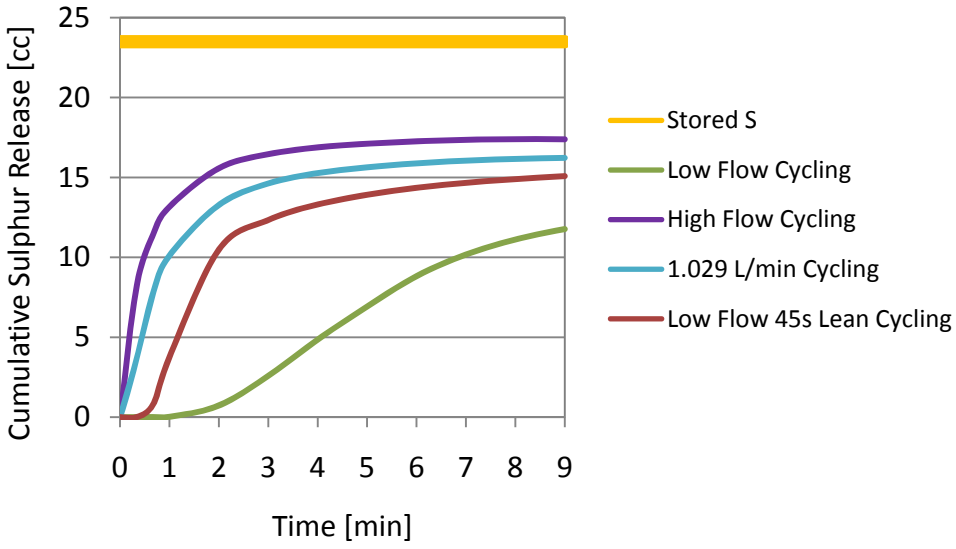

Figure 4.30 Effect of Changes in Low Flow Cycling Flow Rate and Lean Phase Time at 600°C on Cumulative Sulphur Released

An additional experiment was run after the high flow desulphation experiments on the same NxtGen catalyst specimen to determine if residual sulphur remained on the catalyst even after "cleaning" the sample at 700°C in a reductant-rich mixture, as previously suggested in the literature[55,61]. To determine if residual sulphur remained on the catalyst, a repeat at 500°C was performed after the high flow cycling experiments were completed. The exact same amount of sulphur was deposited during poisoning and the desulphation was conducted precisely the same way. Figure 4.31 shows the NO_X performance of the catalyst after depositing sulphur and after the desulphation procedure for both the original experiment and the repeated experiment. Since NO_X slip was higher for the repeated test, the catalyst shows signs of containing residual sulphur. It was assumed that the form of residual sulphur on the catalyst would be quite stable. Although this change occurred after many desulphation experiments, these results show that long term catalyst degradation may occur. Desulphations at higher temperatures than those conducted in

this analysis may be required to fully remove sulphur from the catalyst but would most likely result in unacceptable fuel penalties and severe catalyst degradation.

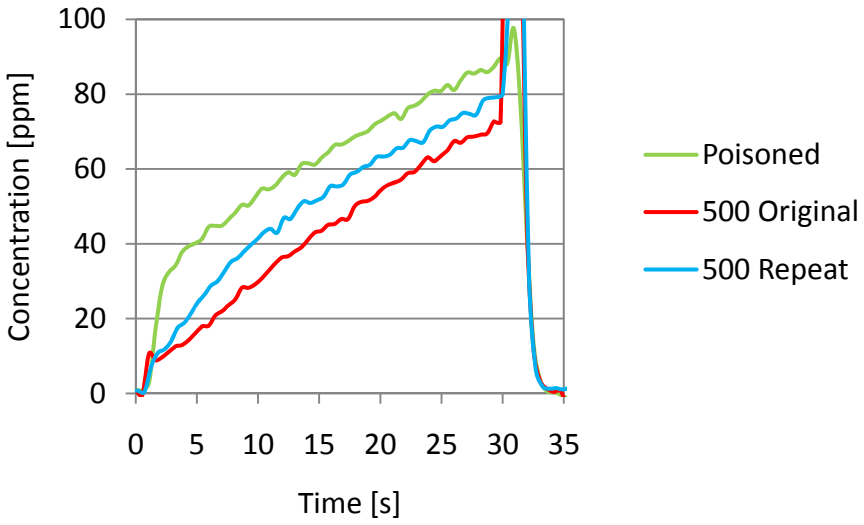

Figure 4.31 NO_X Conversion Comparison Before and After Many Desulphations at 500°C

CONCLUSIONS

Based on the experiments, the most effective reductant for decomposing sulphates and removing sulphur from the catalyst surface was H_2. The presence of CO in the desulphation gas mixture assisted via the formation of more H_2 through the WGS reaction. Additionally, the presence of C_3H_6 in the desulphation gas mixture provided additional H_2 through steam reforming. Furthermore, the presence of both CO_2 and H_2O in the desulphation gas stream decreased the temperature of sulphate stability and assisted in driving the WGS and steam reforming reactions. Overall, the combination of high concentrations of H_2, CO and C_3H_6 in the rich desulphation gas, along with H_2O and CO_2, maximizes the rate of sulphur removal from the catalyst.

An analysis of different desulphation methodologies proved that prolonged reductant gas exposure was more effective than lean/rich cycling in removing sulphur from the catalyst. However, lean/rich cycling is more practical for vehicle applications. Under the conditions tested, high flow cycling achieved a higher rate of sulphur release from the catalyst compared to low flow cycling, even with higher reductant concentration in the low flow gas mixture. Additionally, incremental increases in desulphation temperature under high flow conditions led to proportionally higher releases of sulphur from the catalyst.

Although still suited for single-leg NSR systems, the NxtGen process relies on dual-leg systems. As noted, dual-leg systems operate under low flow regeneration conditions. The results of the low flow experiments showed that the NxtGen desulphation process is dominated by the removal of OSC, meaning that until the surface oxygen is removed, sulphates remain relatively un-

reacted. To ensure optimal operation under dual-leg conditions, a sufficient amount of reductant must be supplied to the catalyst so that the OSC is fully combusted and additional reductant is available for reaction with the sulphate species. Under OSC controlled conditions, there were no significant differences in the amount of sulphur released as a function of temperature above 550^{o}C. Small alterations in the low flow desulphation procedure proved effective for increasing both the rate and degree of sulphate removal. These alterations included decreased lean phase time and slightly increased flow rates. In each case, the goal was to increase the amount of reductant available for reaction with surface sulphates rather than OSC.

It was also determined that the sample contained residual sulphur after high flow cycling experiments had been completed. It was also likely that a variety of sulphates with different stabilities on the catalyst were responsible for many of the sulphur release characteristics. Unless the catalyst composition is known, it remains difficult to determine what sulphate forms are the most stable on the specific catalyst components.

RECOMMENDATIONS

- Investigate the effect of desulphation conducted above 700^{o}C to determine if residual sulphur may be removed without causing severe thermal degradation.

- Determine if significant thermal degradation occurs within the temperatures used, through the use of BET surface area or TEM analysis, to better assess the optimal desulphation temperature.

- Obtain the elemental composition of the catalyst, with permission from NxtGen Emission Controls Inc., in order to associate sulphate stabilities on the catalyst with specific components.

- With permission from NxtGen Emission Controls Inc., perform a microstructural analysis on the catalyst, using a technique such as SEM, to determine the effect of the various desulphation procedures on the catalyst microstructure.

- Compare the results of the desulphation experiments to commercially available catalysts.

- Decrease the catalyst length to evaluate the extent of sulphur re-adsorption down length of the catalyst during desulphation.

- Alter the length of inert phases to determine the effect on overall sulphur release during desulphation cycling.

- Perform a statistical analysis on the data set to determine the degree of acceptable error and further clarify conclusions.

REFERENCES

[1] 2006 air pollutant emissions for Canada (tonnes). April 2008 [cited 17/02/2009]. Available from http://www.ec.gc.ca/pdb/cac/Emissions1990-015/2006/2006_canada_e.cfm (accessed 17/02/2009).

[2] Health effects of air pollution. [cited 17/02/2009]. Available from http://www.hc-sc.gc.ca/ewh-semt/air/out-ext/effe/health_effects-effets_sante-eng.php (accessed 17/02/2009).

[3] *Catalytic converters: Design and durability part I: Chemical principles* 2004. eds. R.M. Heck, S.T. Gulati, M. Khair. Warrendale, PA, USA: SAE International.

[4] *Emission standards reference guide for heavy-duty and nonroad engines.* September 1997. Ann Arbor, MI: United States Environmental Protection Agency, EPA420-F-97-014.

[5] *Heavy-duty engine and vehicle standards and highway diesel fuel sulfur control requirements.* December 2000. Ann Arbor, MI: United States Environmental Protection Agency, EPA420-F-00-057.

[6] Mercedes-Benz firms up launch of three new BlueTEC diesels in US; first AdBlue light-duty vehicles for the US. 2008. *Green Car Congress*2008, sec Diesel.

[7] Control of emissions of hazardous air pollutants from mobile sources; proposed rule. 2000. 65, (No. 151) (August 4, 2000), http://www.epa.gov/otaq/regs/toxics/fr-nprm.pdf (accessed 18/02/2009).

[8] T. Yamauchi, S. Kubo, and S. Yamazaki. 2005. Detailed surface reaction model for three-way catalyst and NO_X storage reduction catalyst. *SAE Technical Paper Series* 2005-01-1112.

[9] N. Miyoshi, S. Matsumoto, K. Katoh, T. Tanaka, J. Harada, N. Takahashi, K. Yokota, M. Sugiura, and K. Kasahara. 1995. Development of new concept three-way catalyst for automotive lean-burn engines. *SAE Technical Paper Series* 950809.

[10] W. Bogner, M. Kramer, B. Krutzsch, S. Pischinger, D. Voigtlander, G. Wenninger, F. Wirbeleit, M.S. Brogan, R.J. Brisley, and D.E. Webster. 1997. Removal of nitrogen oxides from the exhaust of a lean-tune gasoline engine. *Applied Catalysis B: Environmental* 7: 153-171.

[11] W.S. Epling, L.E. Campbell, A. Yezerets, N.W. Currier, and J.E. Parks II. 2004. Overview of the fundamental reactions and degradation mechanisms of NO_X Storage/Reduction catalysts. *Catalysis Reviews* 46, (2): 163-245.

[12] S.S. Mulla, N. Chen, L. Cumaranatunge, G.E. Blau, D.Y. Zemlyanov, W.N. Delgass, W.S. Epling, and F.H. Ribeiro. 2006. Reaction of NO and O_2 to NO_2 on Pt: Kinetics and catalyst deactivation. *Journal of Catalysis* 241: 389-399.

[13] R.L. Muncrief, P. Khanna, K.S. Kabin, and M.P. Harold. 2004. Mechanistic and kinetic studies of NO_X storage and reduction on $Pt/BaO/Al_2O_3$. *Catalysis Today* 98: 393-402.

[14] S. Hodjati, K. Vaezzadeh, C. Petit, V. Pitchon, and A. Kiennemann. 2000. NO_X sorption-desorption study: Application to diesel and lean-burn exhaust gas (selective NO_X recirculation technique). *Catalysis Today* 59: 323-334.

[15] L. Olsson, B. Westerberg, H. Persson, E. Fridell, M. Skoglundh, and B. Anderson. 1999. A kinetic study of oxygen Adsorption/Desorption and NO oxidation over Pt/Al_2O_3 catalysts. *Journal of Physical Chemistry B* 103: 10433-10439.

[16] S. Hodjati, P. Bernhardt, C. Petit, V. Pitchon, and A. Kiennemann. 1998. Removal of NO_X: Part I. Sorption/desorption processes on barium aluminate. *Applied Catalysis B: Environmental* 19: 209-219.

[17] J. Li, J. Theis, W. Chun, C. Goralski, R. Kudla, J. Ura, W. Watkins, M. Chattha, and R. Hurley. 2001. Sulfur poisoning and desulfation of the lean NO_X trap. *SAE Technical Paper Series* 2001-01-2503.

[18] J.R. Theis, J.J. Li, J.A. Ura, and R.G. Hurley. 2002. The desulphation characteristics of lean NO_X traps. *SAE Technical Paper Series* 2002-01-0733.

[19] H. Mahzoul, P. Gilot, J.F. Brilhac, and B.R. Stanmore. 2001. Reduction of NO_X over a NO_X-trap catalyst and the regeneration behaviour of adsorbed SO_2. *Topics in Catalysis* 16/17, (1-4): 293-298.

[20] R. Burch, J.P. Breen, and F.C. Meunier. 2002. A review of the selective reduction of NO_X with hydrocarbons under lean-burn conditions with non-zeolitic oxide and platinum group metal catalysts. *Applied Catalysis B: Environmental* 39: 283-303.

[21] L. Olsson, E. Fridell, M. Skoglundh, and B. Andersson. 2002. Mean field modelling of NO_X storage on $Pt/BaO/Al_2O_3$. *Catalysis Today* 73: 263-270.

[22] K. Shimizu, Y. Saito, T. Nobukawa, N. Miyoshi, and A. Satsuma. 2008. Effect of supports on formation and reduction rate of stored nitrates on NSR catalysts as investigated by in situ FTIR. *Catalysis Today* 139: 24-28.

[23] M. Casapu, J.D. Grunwaldt, M. Maciejewski, and F. Krumeich. 2008. Comparative study of structural properties and NO_X storage-reduction behavior of $Pt/Ba/CeO_2$ and $Pt/Ba/Al_2O_3$. *Applied Catalysis B: Environmental* 78: 288-300.

[24] H. Imagawa, T. Tanaka, N. Takahashi, S. Matsunaga, A. Suda, and H. Shinjoh. 2009. Titanium-doped nanocomposite of Al_2O_3 and ZrO_2- TiO_2 as a support with high sulfur durability for NO_X storage-reduction catalyst. *Applied Catalysis B: Environmental* 86: 63-68.

[25] S. Salasc, M. Skoglundh, and E. Fridell. 2002. A comparison between Pt and Pd in NO_X storage catalysts. *Applied Catalysis B: Environmental* 36: 145-160.

[26] J. Theis, J. Lupescu, J. Ura, and R. McCabe. 2006. Lean NO_X trap system design for cost reduction and performance improvement. *SAE Technical Paper Series* 2006-01-1069.

[27] J.P. Breen, M. Marella, C. Pistarino, and J.R.H. Ross. 2002. Sulfur-tolerant NO_X storage traps: An infrared and thermodynamic study of the reactions of alkali and alkaline-earth metal sulfates. *Catalysis Letters* 80, (3-4): 123-128.

[28] T. Kobayashi, T. Yamada, and K. Kayano. 1997. Study of NO_X trap reaction by thermodynamic calculation. *SAE Technical Paper Series* 970745.

[29] C. Laroo, C. Schenk, B. Olson, P. Way, and M. Joseph. 2002. NO_X adsorber desulfation techniques for heavy-duty on-highway diesel engines. *SAE Technical Paper Series* 2002-01-2871.

[30] I. Tsumagari, H. Hirabayashi, Y. Takenaka, M. Hosoya, and M. Shimoda. 2006. Study of 2-LEG NO_X storage-reduction catalyst system for HD diesel engine. *SAE Technical Paper Series* 2006-01-0211.

[31] Y. Kong, S. Crane, P. Patel, and B. Taylor. 2004. NO_X trap regeneration with an on-board hydrogen generation device. *SAE Technical Paper Series* 2004-01-0582.

[32] S. Matsumoto, Y. Ikeda, H. Suzuki, M. Ogai, and N. Miyoshi. 2000. NO_X storage-reduction catalyst for automotive exhaust with improved tolerance against sulfur poisoning. *Applied Catalysis B: Environmental* 25: 115-124.

[33] *Catalytic converters: Design and durability part II: Mechanical Properties* 2004. eds. R.M. Heck, S.T. Gulati and M. Khair. Warrendale, PA, USA: SAE International.

[34] M.F.L. Johnson. 1990. Surface area stability of aluminas. *Journal of Catalysis* 123: 245-259.

[35] C.-K Loong, J.W. Richardson Jr., and M. Ozawa. 1997. Structural phase transformations of rare-earth modified transition alumina to corundum. *Journal of Alloys and Compounds* 250: 356-359.

[36] D.H. Kim, Y. Chin, G.G. Muntean, A. Yezeretz, N.W. Currier, W.S. Epling, H. Chen, H. Hess, and C.H.F. Peden. 2006. Relationship of Pt particle size to the NO_X storage performance of thermally aged $Pt/BaO/Al_2O_3$ lean NO_X trap catalysts. *Industrial & Engineering Chemistry Research* 45: 8815-8821.

[37] L. Olsson, and E. Fridell. 2002. The influence of Pt oxide formation and Pt dispersion on the reactions $NO_2 \leftrightarrow NO + 1/2\ O_2$ over Pt/Al_2O_3 and $Pt/BaO/Al_2O_3$. *Journal of Catalysis* 210: 340-353.

[38] J. Lee, and H.H. Kung. 1998. Effect of Pt dispersion on the reduction of NO by propene over alumina-supported Pt catalysts under lean-burn conditions. *Catalysis Letters* 51: 1-4.

[39] M. Casapu, J. Grunwaldt, M. Maciejewski, A. Baiker, S. Eckhoff, U. Gobel, and M. Wittrock. 2007. The fate of platinum in $Pt/Ba/CeO_2$ and $Pt/Ba/Al_2O_3$ catalysts during thermal aging. *Journal of Catalysis* 251: 28-38.

[40] D.H. Kim, Y. Chin, J.H. Kwak, J. Szanyi, and C.H.F. Peden. 2005. Changes in Ba phases in BaO/Al_2O_3 upon thermal aging and H_2O treatment. *Catalysis Letters* 105, (3-4): 259-268.

[41] D.H. Kim, J.H. Kwak, J. Szanyi, S.D. Burton, and C.H.F. Peden. 2007. Water-induced bulk $Ba(NO_3)_2$ formation from NO_2 exposed thermally aged BaO/Al_2O_3. *Applied Catalysis B: Environmental* 72: 233-239.

[42] T.J. Toops, B.G. Bunting, K. Nguyen, and A. Gopinath. 2007. Effect of engine-based thermal aging on surface morphology and performance of lean NO_X traps. *Catalysis Today* 123: 285-292.

[43] Workshop regarding regulatory fuels activities. California Environmental Protection Agency Air Resources Board [database online]. 2002 [cited 03/11 2009]. Available from http://www.arb.ca.gov/fuels/gasoline/meeting/2002/ARBPrstn030502.pdf.

[44] I. Hachisuka, H. Hirata, Y. Ikeda, and S. Matsumoto. 2000. Deactivation mechanism of NO_X storage-reduction catalyst and improvement of its performance. *SAE Technical Paper Series* 2000-01-1196.

[45] K. Yoshida, T. Asanuma, H. Nishioka, K. Hayashi, and S. Hirota. 2007. Development of NO_X reduction system for diesel aftertreatment with sulfur trap catalyst. *SAE Technical Paper Series* 2007-01-0237.

[46] A. Amberntsson, M. Skoglundh, M. Jonsson, and E. Fridell. 2002. Investigations of sulphur deactivation of NO_X storage catalysts: Influence of sulphur carrier and exposure conditions. *Catalysis Today* 73: 279-286.

[47] P. Engstrom, A. Amberntsson, M. Skoglundh, E. Fridell, and G. Smedler. 1999. Sulphur dioxide interaction with NO_X storage catalysts. *Applied Catalysis B: Environmental* 22: L241-L248.

[48] J.D. Wilde, and G.B. Marin. 2000. Investigation of simultaneous adsorption of SO_2 and NO_X on Na-γ-alumina with transient techniques. *Catalysis Today* 62: 319-328.

[49] E. Fridell, A. Amberntsson, L. Olsson, A.W. Grant, and M. Skoglundh. 2004. Platinum oxidation and sulphur deactivation in NO_X storage catalysts. *Topics in Catalysis* 30/31, (July): 143-146.

[50] H. Mahzoul, L. Limousy, J.F. Brilhac, and P. Gilot. 2000. Experimental study of SO_2 adsorption on barium-based NO_X adsorbers. *Journal of Analytical and Applied Pyrolysis* 56: 179-193.

[51] Y. Takahashi, Y. Takeda, N. Kondo, and M. Murata. 2004. Development of NO_X trap system for commercial vehicle - basic characteristics and effects of sulfur poisoning -. *SAE Technical Paper Series* 2004-01-0580.

[52] M. Al-Harbi. 2008. Environmental technology management (ETM): Performance and reaction activity changes of a NO_X Storage/Reduction catalyst as a function of regeneration mixture and thermal degradation. MASc., University of Waterloo.

[53] J.A. Ura, C.T. Goralski Jr., G.W. Graham, R.W. McCabe, and J.R. Theis. 2005. Laboratory study of lean NO_X trap desulfation strategies. *SAE Technical Paper Series* 2005-01-1114.

[54] D.H. Kim, J.H. Kwak, X. Wang, J. Szanyi, and C.H.F. Peden. 2008. Sequential high temperature reduction, low temperature hydrolysis for the regeneration of sulfated NO_X trap catalysts. *Catalysis Today* 136: 183-187.

[55] S. Poulston, and R.R. Rajaram. 2003. Regeneration of NO_X trap catalysts. *Catalysis Today* 81: 603-610.

[56] M. Molinier. 2001. NO_X adsorber desulfurization under conditions compatible with diesel applications. *SAE Technical Paper Series* 2001-01-0508.

[57] Z. Liu, and J.A. Anderson. 2004. Influence of reductant on the regeneration of SO_2-poisoned $Pt/Ba/Al_2O_3$ NO_X storage and reduction catalyst. *Journal of Catalysis* 228: 243-253.

[58] C.C. Chang. 1978. Infrared studies of SO_2 on γ-alumina. *Journal of Catalysis* 53: 374-385.

[59] R.J. Ferm. 1957. The chemistry of carbonyl sulfide. *Chemical Reviews* 57, (4): 621-640.

[60] D.R. Monroe, and W. Li. 2002. Desulfation dynamics of NO_X storage catalysts. *SAE Technical Paper Series* 2002-01-2886.

[61] D.H. Kim, J. Szanyi, J.H. Kwak, T. Szailer, J. Hanson, M.C. Wang, and C.H.F Peden. 2006. Effect of barium loading on the desulfation of Pt-BaO/Al_2O_3 studied by H_2 TPRX, TEM, sulfur K-edge XANES, and in situ TR-XRD. *Journal of Physical Chemistry B* 110: 10441-10448.

[62] S.Y. Jung, S.J. Lee, T.J. Lee, C.K. Ryu, and J.C. Kim. 2006. H_2S removal and regeneration properties of Zn-Al-based sorbents promoted with various promoters. *Catalysis Today* 111: 217-222.

APPENDIX A – AUXILIARY FIGURES

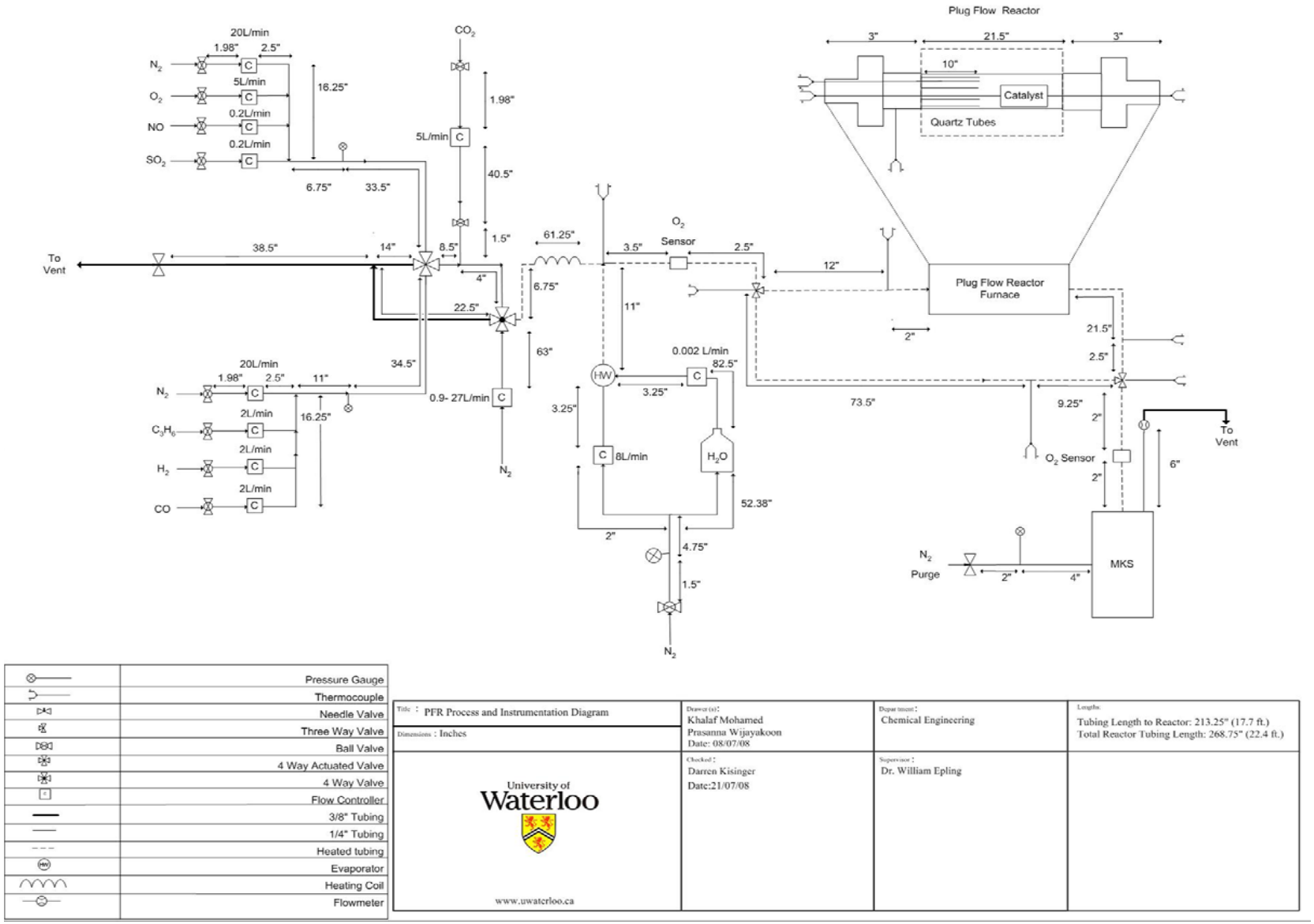

Figure A.1 PFR Reactor Process and Instrumentation Diagram